Atmos. Chem. Phys., 22, 6365–6391, 2022
https://doi.org/10.5194/acp-22-6365-2022

Atmospheric Chemistry and Physics
Open Access
EGU

An evaluation of new particle formation events in Helsinki during a Baltic Sea cyanobacterial summer bloom

Roseline C. Thakur[1], Lubna Dada[1,2,3], Lisa J. Beck[1], Lauriane L. J. Quéléver[1], Tommy Chan[1], Marjan Marbouti[1,11], Xu-Cheng He[1], Carlton Xavier[1], Juha Sulo[1], Janne Lampilahti[1], Markus Lampimäki[1], Yee Jun Tham[1,10], Nina Sarnela[1], Katrianne Lehtipalo[1,4], Alf Norkko[7,8], Markku Kulmala[1,5,6], Mikko Sipilä[1], and Tuija Jokinen[1,9]

[1]Institute for Atmospheric and Earth System Research/Physics, Faculty of Science, University of Helsinki, 00014 Helsinki, Finland
[2]School of Architecture, Civil and Environmental Engineering, École Polytechnique Fédérale de Lausanne, 1951 Lausanne, Switzerland
[3]Laboratory of Atmospheric Chemistry, Paul Scherrer Institute, 5232 Villigen PSI, Switzerland
[4]Finnish Meteorological Institute, 00560 Helsinki, Finland
[5]Aerosol and Haze Laboratory, Beijing Advanced Innovation Center for Soft Matter Science and Engineering, Beijing University of Chemical Technology, 100089 Beijing, China
[6]Joint International Research Laboratory of Atmospheric and Earth System Sciences, Nanjing University, 210023 Nanjing, China
[7]Tvärminne Zoological Station, University of Helsinki, J. A. Palméns väg 260, 10900 Hanko, Finland
[8]Baltic Sea Centre, Stockholm University, 10691 Stockholm, Sweden
[9]Climate & Atmosphere Research Centre (CARE-C), The Cyprus Institute, P.O. Box 27456, Nicosia, 1645, Cyprus
[10]School of Marine Sciences, Sun Yat-Sen University, 519082 Zhuhai, China
[11]Department of Electronics and Nanoengineering, Aalto University, 00076 Aalto, Finland

Correspondence: Roseline C. Thakur (roseline.thakur@helsinki.fi)

Received: 27 August 2021 – Discussion started: 4 October 2021
Revised: 22 February 2022 – Accepted: 31 March 2022 – Published: 17 May 2022

Abstract. Several studies have investigated new particle formation (NPF) events from various sites ranging from pristine locations, including forest sites, to urban areas. However, there is still a dearth of studies investigating NPF processes and subsequent aerosol growth in coastal yet semi-urban sites, where the tropospheric layer is a concoction of biogenic and anthropogenic gases and particles. The investigation of factors leading to NPF becomes extremely complex due to the highly dynamic meteorological conditions at the coastline especially when combined with both continental and oceanic weather conditions. Herein, we engage in a comprehensive study of particle number size distributions and aerosol-forming precursor vapors at the coastal semi-urban site in Helsinki, Finland. The measurement period, 25 June–18 August 2019, was timed with the recurring cyanobacterial summer bloom in the Baltic Sea region and coastal regions of Finland. Our study recorded several regional/local NPF and aerosol burst events during this period. Although the overall anthropogenic influence on sulfuric acid (SA) concentrations was low during the measurement period, we observed that the regional or local NPF events, characterized by SA concentrations on the order of 10^7 molec. cm^{-3}, occurred mostly when the air mass traveled over the land areas. Interestingly, when the air mass traveled over the Baltic Sea, an area enriched with algae and cyanobacterial blooms, high iodic acid (IA) concentration coincided with an aerosol burst or a spike event at the measurement site. Further, SA-rich bursts were seen when the air mass traveled over the Gulf of Bothnia, enriched with cyanobacterial blooms. The two most important factors affecting aerosol precursor vapor concentrations, and thus the aerosol formation, were speculated to be (1) the type of phytoplankton species and

intensity of bloom present in the coastal regions of Finland and the Baltic Sea and (2) the wind direction. During the events, most of the growth of sub-3 nm particles was probably due to SA, rather than IA or methane sulfonic acid (MSA); however much of the particle growth remained unexplained indicative of the strong role of organics in the growth of particles, especially in the 3–7 nm particle size range. Further studies are needed to explore the role of organics in NPF events and the potential influence of cyanobacterial blooms in coastal locations.

1 Introduction

New particle formation (NPF) and the growth of aerosols are regional processes occurring globally, introducing a substantial aerosol load into the atmosphere. NPF has been observed in different environments, including pristine environments (Asmi et al., 2016; Jang et al., 2019; Jokinen et al., 2018), polluted boundary layers and urban areas (Kulmala et al., 2016, 2017, 2021; Manninen et al., 2010; Wang et al., 2017; Cai and Jiang, 2017; Deng et al., 2020; Yao et al., 2018; Du et al., 2021; Yan et al., 2021), boreal forests (Buenrostro Mazon et al., 2016; Dada et al., 2017; Kulmala et al., 2013; Kyrö et al., 2014; Leino et al., 2016; Nieminen et al., 2014; Rose et al., 2018), tropical forests (Artaxo et al., 2013; Wimmer et al., 2018), and mountaintops (Bianchi et al., 2016, 2020). Few studied the coastal environment, although the coastal NPF research started quite early. The investigation of coastal aerosol events dates back to 1978, when the measurements of total aerosol number concentration were carried out at the Tasmanian coast (Bigg and Turvey, 1978). After that atmospheric nucleation was observed in the Southern Hemisphere around the Antarctic coastline (O'Dowd et al., 1997), in Mace Head (Flanagan et al., 2005; McFiggans et al., 2004; O'Dowd et al., 2002), in coastal regions of China and Spain (Yu et al., 2019; Mc Figgans et al., 2010; Mahajan et al., 2011), and in open-water regions of northeastern Greenland (Dall'Osto et al., 2018). Most of these studies have identified biogenic emissions from marine algae as the main precursors driving the new particle formation in a perfect coastal setting.

The measurements of gaseous precursors, meteorology and biogenic influences are important to study the coastal NPF, which may lead to the formation of coastal/marine clouds. Coastal clouds are the drivers of many coastal ecosystems (Carbone et al., 2013; Emery et al., 2018; Lawson et al., 2018). Any impact or fluctuations in the cloud formation may impact several other processes of the fragile coastal ecosystem. These coastal clouds demonstrate a high sensitivity to CCN (cloud condensation nuclei; He et al., 2021b), and they have a significant impact on the radiation budget because they have a high infrared emission and albedo when compared to the dark waterbodies down below. In this study we highlight the type of NPF processes and their drivers in a semi-urban coastal setting where the atmosphere could be a mixture of anthropogenic and biogenic emissions. Unlike the abovementioned previous studies which were mostly carried out in perfect coastal environments where NPF would be most likely affected by the biogenic emissions, this study helps to evaluate the impact of urban emissions vs. coastal emissions on NPF and the cloud formation processes at large.

It is well documented that sulfuric acid (henceforth SA) is an important precursor to NPF in most environments (Almeida et al., 2013; Kulmala et al., 2013; Croft et al., 2016; Jokinen et al., 2017; Kirkby et al., 2011; Sipilä et al., 2010). The advancement in aerosol research revealed that a binary system of SA and water is not sufficient to produce particles in ambient atmospheric conditions without stabilizing compounds (Benson et al., 2008; Duplissy et al., 2016; Kirkby et al., 2011). More recently, it has been found that a ternary system involving SA–ammonia–water or SA–amine–water yields much higher nucleation rates as compared to the binary system (Kulmala et al., 2000; Benson et al., 2008; Almeida et al., 2013; Glasoe et al., 2015; Kürten et al., 2016). In addition to these systems, organic compounds which are highly oxygenated – thus less volatile – have been found to contribute to secondary organic aerosol (SOA) mass in forested areas, mountaintops and anthropogenically influenced field sites (Ehn et al., 2014; Pierce et al., 2011; Riipinen et al., 2012; Zhang et al., 2009; Heikkinen et al., 2020; Bryant et al., 2020), and laboratory experiments have shown that they can contribute also to the first steps of NPF (Simon et al., 2020; Lehtipalo et al., 2018; Kirkby et al., 2016; Tröstl et al., 2016).

Furthermore, another important molecular class, iodine, as well as its related oxidized species, plays a crucial role in NPF especially in coastal areas (Allan et al., 2015; Mahajan et al., 2009; Raso et al., 2017; Sipilä et al., 2016) and in pristine marine locations (Baccarini et al., 2020; Beck et al., 2021; He et al., 2021b). Some previous studies have reported the emissions of I_2 from the macroalgae at coastal sites (Huang et al., 2010; Peters et al., 2005; Saiz-Lopez and Plane, 2004). Several studies from coastal sites like Roscoff, France (Mahajan et al., 2009; McFiggans et al., 2010); Mace Head, Ireland (O'Dowd et al., 2002); and other European coastlines (Mahajan et al., 2011; Saiz-Lopez et al., 2012) have reported iodine species initiating NPF. The reported events can be considered aerosol burst events with high aerosol concentration and exceptionally high initial growth rates (GRs; O'Dowd et al., 2002; McFiggans et al., 2004; Mahajan et al., 2011). The study from the Roscoff coast suggests that the daytime emissions of I_2 produced by macroalgae during low tides drives the particle formation (McFiggans et al., 2010). The iodine oxides and/or oxoacids formed

by the biogenic emissions from the micro- and macroalgae near the coastal regions are capable of self-clustering, which could form new particles with a diameter < 3 nm and sometimes with a high gas concentration reaching up to 10^6 cm^{-3} or even more. Recent studies have shown that ion-induced IA nucleation proceeds at the kinetic limit and that the overall nucleation rates (ion-induced nucleation and neutral nucleation) driven by iodine oxoacids (IA and iodous acid, HIO_2) are high, even exceeding the rates of well-known precursors of NPF (He et al., 2021a, b): SA with roughly 100 pptv ammonia under similar conditions (Sipilä et al., 2010). The rapid photolysis of I_2 (< 10 s) produces I atoms above the ocean surface and can be detected in high concentrations close to the source region (McFiggans et al., 2010). However, the compounds with longer lifetimes such as CH_3I (2 d) provide a source of iodine throughout the troposphere (Saiz-Lopez et al., 2012).

Dimethyl sulfide (DMS) oxidation by an OH radical in the daytime and by nitrate radical in the nighttime yields other aerosol precursor gases, such as methane sulfonic acid (henceforth, MSA) and SA (Barnes et al., 2006), which play a crucial role in the NPF processes. In a marine coastal environment, MSA concentrations, which are typically lower than those of SA, could be as low as 10 % of SA concentration and could maximally reach 100 % of SA concentration (Eisele and Tanner, 1993), yet MSA is a potential candidate to participate in the atmospheric nucleation and growth processes (Beck et al., 2021). The stability of heterogeneous MSA clusters have been studied in laboratory and modeling studies (Chen et al., 2020, 2016, 2015), but no study has yet documented MSA clusters in the field. The limited NPF studies in the semi-urban coastal regions and the dynamic coastal meteorology drives the motivation of this research. Another motivation for this research is that to date no detailed studies on the impact of biogenic emissions on NPF events in Finland have been done before, despite the fact that extensive cyanobacterial blooms occur every year in the Baltic Sea region and neighboring waterbodies (including Finnish lakes) (Kahru and Elmgren, 2014), which could be a significant source of iodine species, SA and MSA. Increasing temperatures and the excessive nutrient load in the Baltic Sea promote algal growth (Kuosa et al., 2017; Suikkanen et al., 2007, 2013). According to HELCOM (Helsinki Commission; Baltic Marine Environment Protection Commission), the Baltic Sea has warmed 0.3 °C per decade; however after 1990 it became significantly faster at 0.6 °C per decade, and in Finnish coastal areas the warming is even faster with a 2 °C increase since 1990 (Humborg et al., 2019). The amount of blue-green algae (i.e., cyanobacteria) has shown a statistically significant increase in open-sea areas in the Gulf of Finland, the Sea of Åland and the Sea of Bothnia in the last 40 years (Kahru and Elmgren, 2014). The increase in frequency and intensity of cyanobacterial blooms would increase the potential emission of biogenic gases changing the composition of the overlying atmosphere and the atmosphere of the neighboring sites, depending on the meteorological conditions. In this semi-urban coastal setting the concentration of gaseous precursors and aerosol size distribution may be influenced by the local meteorological parameters such as wind direction, wind speed and air mass turbulence especially at the surface layer of the lower atmosphere. Coastal locations are dynamic environments with rapid changes in meteorological parameters, also making the study of NPF more challenging.

In this study, we aim at producing a thorough evaluation of aerosol precursor molecules with a detailed analysis of NPF events during the cyanobacterial bloom period, in the coastal city of Helsinki, Finland, from June to August (summer) 2019. This work evaluates the role of phytoplankton blooms and meteorological parameters in the NPF events observed during the measurement period. We also identify the major precursor vapors and molecular clusters found during the aerosol events. Here, we formulate the hypothesis that gaseous precursors formed from the biogenic emissions from the surrounding marine areas could play an important role in the nucleation processes in Helsinki. Although Helsinki is a coastal area, the role of marine emissions on NPF processes has not been studied before.

2 Measurement site and methodology

The measurement sites are surrounded by coastal waterbodies (< 4 km, Vanhankaupunginselkä), forests (< 3 km) and a road connecting to the main city (< 300 m) as seen in Fig. 1. Overall Helsinki is located on relatively flat land on the coast of the Gulf of Finland. The Helsinki metropolitan area is about 765 km^2 with approximately 1 million inhabitants, counting together the city of Helsinki and the neighboring cities of Espoo, Vantaa and Kauniainen. The climate in southern Finland can be classified as either marine or continental depending on the air flows and pressure systems. Either way, the weather is milder than typical at the same latitude (60° N) mainly due to the Atlantic Ocean and the warm Gulf Stream.

The site and measurement period (25 June–18 August 2019) selected for this particular study are unique, since this semi-urban location could be influenced by emissions from the recurring summertime blooms in the Baltic Sea and the neighboring coastal regions. As per the SYKE press release (Finnish Environment Institute; 2019) the northern part of the Baltic Sea's main basin, the entrance to the Gulf of Finland and south of the Åland Islands were enriched with blue-green algae (cyanobacteria). The bloom lasted from June–August 2019. In coastal areas, bloom was mostly spotted in the Archipelago Sea, Gulf of Finland, Bothnian Sea and the Quark. The bloom situation developed rapidly and spatially highly variable, even over short distances. The fragmented nature of the coastal areas and changing wind and water currents make the algal bloom conditions highly dynamic.

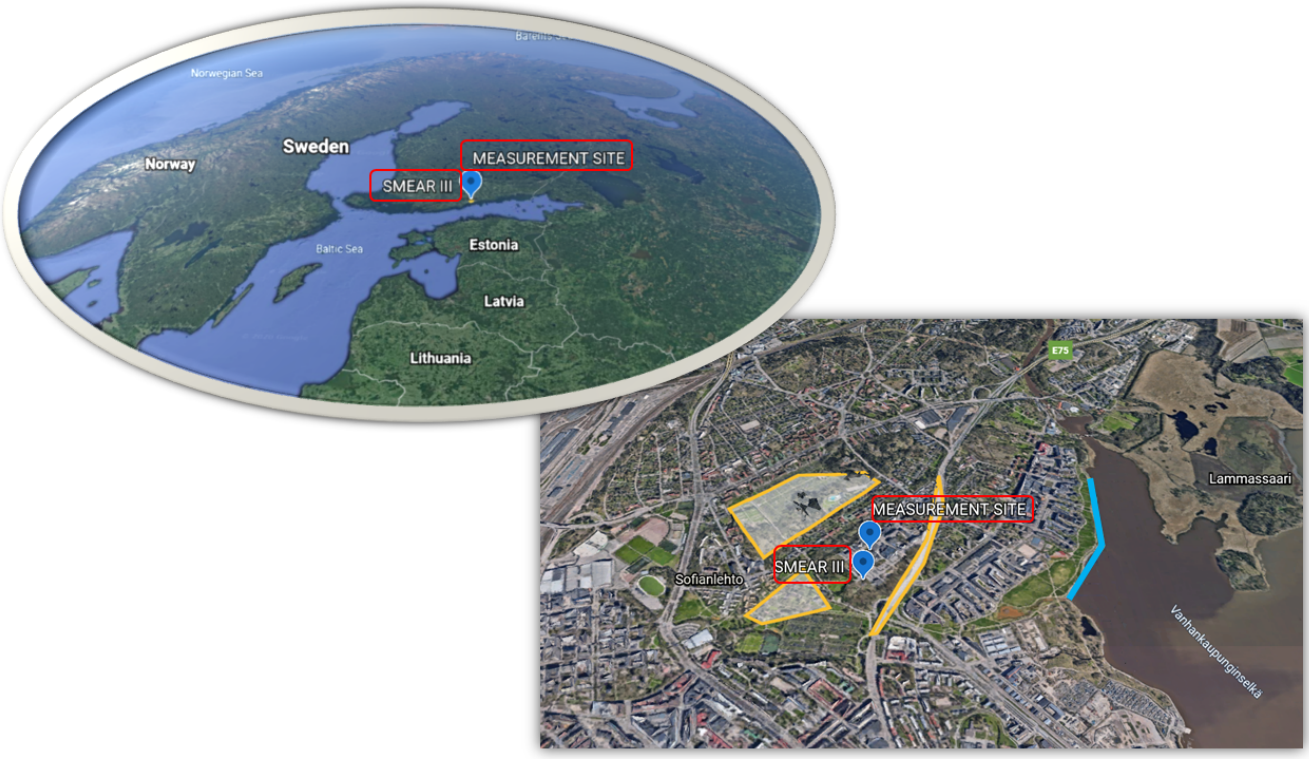

Figure 1. Map showing the two locations included in the study where instruments were operated (upper-left panel). The yellow polygons on the left side of the measurement locations (in the lower-right panel) show forest and park areas with little or no traffic (west and northwest, 300 m from the measurement site). The yellow double lines to the right of the measurement locations are the traffic area of the main road (E75) leading to the Helsinki city center (250 m east of the measurement site). The blue lines depict the coastline after which the lakes and coastal waters of the Gulf of Finland start (1 km to the east from the measurement site). © Google Earth 2019.

Main instruments

To understand the chemical composition of the precursor vapors emitted from various sources around the site, the chemical ionization–atmospheric pressure interface–time of flight mass spectrometer (CI–APi–TOF) was operated from the fourth floor laboratory of the Physicum building, Kumpula campus, University of Helsinki (60°12′ N, 24°58′ E; 49 m a.m.s.l.). The other aerosol and trace gases instruments were operated at the SMEAR III (Station for Measuring Ecosystem–Atmosphere Relations, 60.20° N, 24.96° E; 25 m a.m.s.l.), which is 180 m away from the mass spectrometric measurement site.

The atmospheric pressure interface–time of flight (APi–TOF) mass spectrometer is the state-of-the-art instrument for gas phase chemical composition investigations including aerosol precursor characterizations. Here the instrument is coupled with a nitrate-based chemical ionization (CI) inlet in order to measure neutral gas phase molecules that are clustered and charged with a reagent ion. In our study we used inlet design as described by Eisele and Tanner (1993) and Kurten et al. (2011) and further used by Jokinen et al. (2012). The time of flight (TOF) mass analyzer can detect molecules with masses up to 2000 Th (Thomson) with a mass resolution of 3600 Th Th^{-1}. More details on the working principle of the instrument and calibrations can be found in earlier studies (Junninen et al., 2010; Jokinen et al., 2012; Kürten et al., 2014). The sampled air was drawn in through a 1 m long, 3/4 in. diameter stainless-steel tube with an average flow rate of 10 L min^{-1}. In this study, the chemical ionization was done via nitrate ions (NO_3^-) through X-ray exposure of nitric acid (HNO_3, flow rate: 3 mL min^{-1}), saturating the sheath airflow entering the CI (flow rate: 30 L min^{-1}); the inlet flow of 10 L min^{-1} was reached by using a 40 L min^{-1} total flow. The instrument was calibrated prior to the experiment according to (Kürten et al., 2012), resulting in a calibration factor of 1.45×10^9 molecules per normalized unit signal including the diffusion losses in the inlet line.

The resulting data (i.e., obtained signals) were averaged to 60 min before the mass calibration step performed through the MATLAB-based program tofTools (Junninen et al., 2010). SA, MSA and IA concentrations are calculated after normalizing them with the reagent ions (NO_3^- and $(HNO_3)NO_3$) using the equation mentioned in Jokinen et al. (2012). The uncertainty range of the measured concentrations reported in this study was estimated to be −50 % to +100 %, and the limit of detection (LOD) was 4 ×

10^4 molec. cm^{-3} (Jokinen et al., 2012). HOMs (highly oxygenated organic molecules) and IA have been estimated to be charged similarly at a kinetic limit similar to SA (Ehn et al., 2014; Sipilä et al., 2016), so the calibration factor for them should be similar, but please note that the concentration of compounds other than SA can be highly uncertain due to different ionizing efficiencies, sensitivities and other unknown uncertainties. If MSA, IA or HOMs do not ionize at the kinetic limit, these concentrations could be underestimated, and thus, the concentrations reported here should be taken as low limit values. The normalized signals of specific HOMs found in the study are calculated using high-resolution peak-fitting data. Please note that the concentration of highly oxygenated molecules (sum of all HOMs, monomers and dimers) was calculated from the unit mass resolution data.

A Neutral cluster and Air Ion Spectrometer (NAIS, Airel Ltd., Estonia; Manninen et al., 2010; Mirme and Mirme, 2013) was used to measure the number size distribution of both positive and negative ions between 0.8 and 42.0 nm (electric mobility diameter). The NAIS also measures the number size distribution of total particles (neutral) between 2.5–42.0 nm. The NAIS consists of two multichannel electrical differential mobility analyzer (DMA) columns operating in parallel. The columns differ by the polarity of the ions measured but are otherwise identical (Mirme and Mirme, 2013) in operation. However they may differ in the transfer functions after calibration. The calibration procedure for the DMAs is presented in Mirme and Mirme (2013). The ion mode measurements are corrected as in Wagner et al. (2016). The flow rate of the instrument is 60 L min^{-1}, which is split into 30 L min^{-1} for each DMA. The instrument was installed in the SMEAR III station. The data were recorded every 2 s.

Larger particles of 3–820 nm were measured using a twin differential mobility particle sizer (DMPS) (Aalto et al., 2001). The instrument was installed in the SMEAR III station. The time resolution of data is 10 min.

The size distribution of 1–3 nm particles was measured by a particle size magnifier (PSM, Airmodus Ltd., Finland; Vanhanen et al., 2011) in series with a condensation particle counter (Airmodus Ltd., Finland). The PSM was operated by scanning the flow at 0.1–1.3 L min^{-1} (continuously changing the saturator flow rate), which allows for determining the 1–3 nm particle concentration and calculating the particle size distribution. The data were recorded for each second, and the duration of each scan was fixed to 240 s. The raw data inversion was carried out through the kernel method (Chan et al., 2020; Lehtipalo et al., 2014). The raw data of the PSM employed a pretreatment filter that calculates the correlation between the observed particle concentration and the saturator flow rate of a single scan and discards scans with significant non-correlation or negative correlation (Chan et al., 2020). Details about the back-trajectory calculations, Chl *a* data analysis, and meteorological and other calculations of parameters such as growth rates and formation rates are explained in the Supplement.

3 Results and discussions

3.1 Meteorological parameters and cyanobacterial bloom during the study

3.1.1 Meteorological parameters

The meteorological parameters, especially the wind speed, wind direction and ambient temperature, varied significantly during the study period. The time zone in the entire study is UTC+2. This study period includes the hottest summer days of Finland in the year 2019. The average temperature during 17–28 July 2019 (the warmest period) was 21.6 °C with a maximum temperature of 31.6 °C recorded on the 28 July 2019 (Fig. 2). The temperature started to decrease after 29 July 2019. The average temperature in August was 16.5 °C with a maximum temperature of 21.9 °C recorded on 5 August 2019.

The wind direction was highly variable during the June–July period. The wind direction in July was mostly from the sectors 270–320° (west to northwest) and 90–150° (east to southeast). In August, the wind gained more stability and was dominantly blowing from 180–270° (south to west) (Fig. 2). The wind speed also showed high variability in June–July. The wind speeds during June and early weeks of July were mostly $> 6.5\,m\,s^{-1}$, followed by a bit calmer mid-July (mostly $\leq 4\,m\,s^{-1}$) with preceding high winds in end of July until mid-August (gusts of winds $> 5.2\,m\,s^{-1}$) (Fig. 2). However, the average wind speeds in both the months was $3\,m\,s^{-1}$. The average daylight hours in July were 17–18 h with the daytime hours between 04:00–22:00, which starts to decrease in August to 15–16 h of daylight per day (05:00–21:00) as per the global radiation data obtained from the SMEAR III station for the study period. Therefore, the actual nighttime hours in our measurement site can be considered from 23:00–03:00 during Finnish summers.

3.1.2 Cyanobacterial-bloom conditions during the study

The Baltic Sea (defined as 53–66° N, 10–30° E including the Gulf of Bothnia, Gulf of Finland and Gulf of Riga) is usually characterized by two algal blooms, one occurring in early spring (mostly diatoms) and then a summer bloom increasingly dominated by cyanobacteria (blue-green algae). The summer bloom period selected for this study was typically characterized by cyanobacteria. When these microscopic cyanobacteria multiply and aggregate, they are seen as blue-green patches or scum-like layers over the surface of lakes and marine waters. The warm early-summer temperatures (during June) resulted in a cyanobacterial bloom (Finnish national monitoring; SYKE press release, 2019). However, the weather conditions at the end of July began changing with high winds causing the cyanobacteria to be highly mixed in

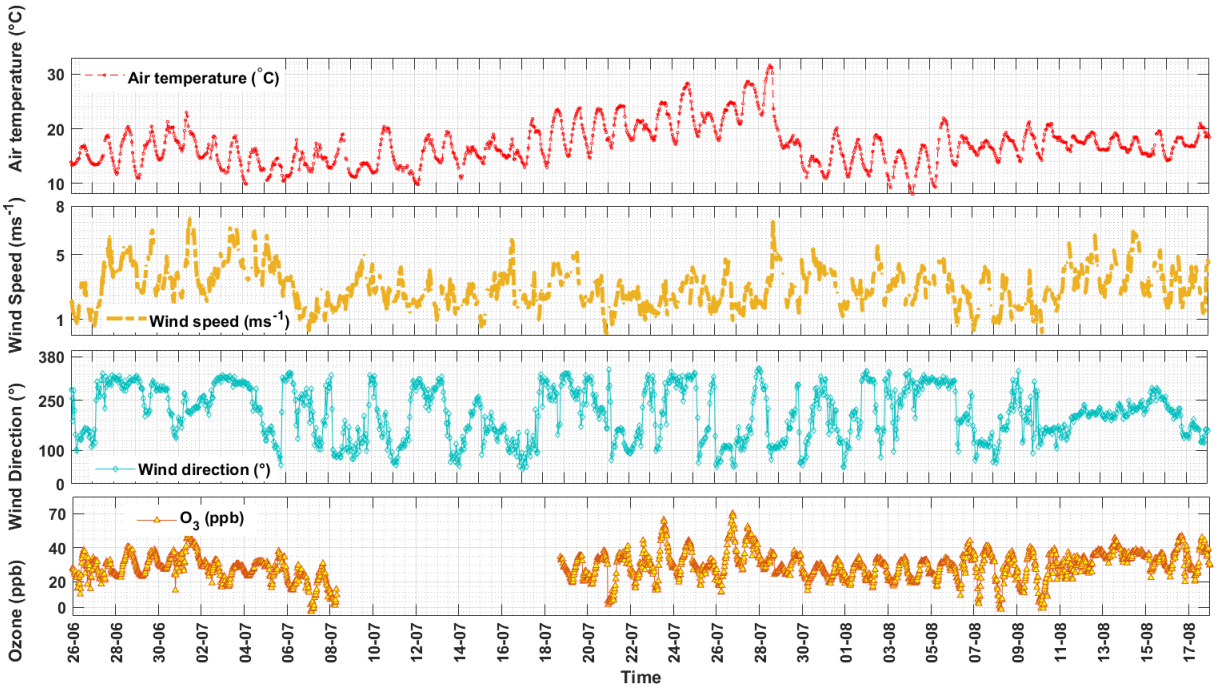

Figure 2. Time series of meteorological parameters and O_3 concentration (data from the SMEAR III station, 30 min averaged) during the study period.

the water column, which reduced bloom intensity at the sea surface to lower-than-normal mean cyanobacterial biomass (mean biomass of cyanobacteria: 105 µg L^{-1}, Kownacka et al., 2020) at the end of July and August (SYKE press release, 2019). However the average biomass of cyanobacteria in 2019 (196 µg L^{-1}, Kownacka et al., 2020) was slightly higher than the average. Subsequently, temperatures were lower in August as compared to June and July and windier as compared to other summer months. These windy conditions kept the lake cyanobacteria well mixed in the water. The northern Baltic Sea, including the Gulf of Finland, the southern parts of the Åland Islands and even the Bothnian Sea, occasionally observed massive blooms of cyanobacteria during June–August 2019. However, the bloom intensity of cyanobacteria at the coastal areas was intermittent and changed rapidly due to the spatial complexity of the coastline and variable winds and currents.

These cyanobacterial blooms are generally dominated by three taxa, *Nodularia spumigena*, *Aphanizomenon* sp. and *Dolichospermum* sp. (Knutson et al., 2016; Kownacka et al., 2020). In the Baltic Sea, these cyanobacteria actually contribute the most to the total pelagic nitrogen fixation (Klawonn et al., 2016). Other potential primary producers emitting vapors are the littoral macroalgae growing along the shallow coastline. For example, the perennial macroalgae *Fucus vesiculosus* cover large areas of the coastal areas of Baltic Sea, where they support very high biomass and high productivity (Attard et al., 2019). Low sea levels (0.2–0.8 m, wave height at the Suomenlinna aaltopoiju station at https://en.ilmatieteenlaitos.fi/wave-height, last access: 21 November 2021) were recorded in mid-July (11–27 July 2019) during the period when high temperatures (20 °C and above) prevailed (Fig. 2) in our study region. During these conditions, contributors to emissions might be a mix of both coastal macroalgae and open-sea microalgae, which are mostly the cyanobacteria. There is a possibility that reasonably large extents of coastal macroalgae, including *F. vesiculosus*, were exposed to direct sunlight (in shallow waters or low-tide conditions) during the decay of the blooms during mid-August (when the bloom intensity was low, SYKE press release, 2019), hence making this time window favorable for observing potentially high emissions in gas phase from the macroalgae, in addition to the emissions from cyanobacterial blooms. However, in the semi-urban coastal setting of this measurement site, there could be various other parameters which could also play a role in determining the concentrations of the biogenic emissions, for example, the wind speed and wind direction. The atmosphere in this semi-urban coastal location is itself a cocktail of various vapors, oxidants and particles, which would affect the quantification, source apportionment and characterization of the biogenic emissions.

3.2 Precursor vapor concentrations and their sources

The measured daytime precursor vapor concentrations showed a regular diurnal cycle consistent with the photochemical production of SA and IA in 90 % of the days in

this study. SA, the key precursor of atmospheric NPF, is formed mainly by a reaction of sulfur dioxide with OH radicals, which is predominantly controlled by the photochemical cycles (Sipilä et al., 2010; Jokinen et al., 2017). The daily mean concentration of SA in July and August were almost similar, $\sim 3 \times 10^6$ molec. cm^{-3}. The mean concentration is slightly lower as compared to the concentrations of SA measured in a Helsinki street canyon, 1×10^7 molec. cm^{-3} (Olin et al., 2020), but similar to the SA concentration measured at the SMEAR III station in 2018 (Okuljar et al., 2021). In the study of Olin et al. (2020), SA concentrations were greatly affected by vehicular traffic, as the site is situated at a busy street canyon. The SMEAR III station is considered a background site much less affected by vehicular traffic (Okuljar et al., 2021). In comparison to other locations, the daytime SA concentration has been reported to be from 10^5 up to 10^7 molec. cm^{-3} in a pristine Antarctic region (Mauldin et al., 2001; Jokinen et al., 2018); 10^6 molec. cm^{-3} in remote continental, remote marine and forest regions; and 10^7 molec. cm^{-3} in urban and rural agricultural lands using the same technique as here (Berresheim et al., 2000; Kuang et al., 2008; Petäjä et al., 2009; Kurtén et al., 2011; Zheng et al., 2011; Chen et al., 2012; Jokinen et al., 2012, 2017; Kürten et al., 2014; Bianchi et al., 2016; Baalbaki et al., 2021; Dada et al., 2020). It has been well documented that SA contributes to aerosol formation and growth processes (Boy et al., 2008; Eisele et al., 2006; Fiedler et al., 2005; Iida et al., 2008; Sarnela et al., 2015; Jokinen et al., 2018; Kürten et al., 2015, 2016; Mauldin et al., 2001; Paasonen et al., 2010; Wang et al., 2011; Weber et al., 1998, 1999; Yao et al., 2018; Dada et al., 2020). Most of these studies are conclusive that SA concentration in the atmosphere depends on the anthropogenic and biogenic activities around the site.

In the coastal marine boundary layer, the MSA concentration is typically 10 %–100 % of that of SA (Berresheim et al., 2002; Eisele and Tanner, 1993). Until recently, no studies have been found to report MSA and IA concentrations in a coastal urban setting of Finland. The daily mean concentration of MSA in July and August was almost similar, 4×10^5 molec. cm^{-3}. The mean concentration of IA in July and August was 1×10^6 and 3×10^6 molec. cm^{-3}, respectively, showing an increase of 2 times in IA concentrations in August (Fig. S1 in the Supplement). A similar increase in IA concentrations from summer to autumn was observed in the Arctic Ocean, where the increase in IA was attributed to the freezing onset of the pack ice and increase in ozone concentrations (Baccarini et al., 2020). However, here the increase is mainly due to the change in the air mass arriving at the experimental site, enriched with biogenic emissions from the blooms. For the same period, the CI–APi–TOF data show exceptionally high concentrations of highly oxygenated organic molecules (HOMs), with monomer concentrations (300–450 Da) of 10^8 molec. cm^{-3} and HOM dimer concentrations (450–600 amu) of 10^8 molec. cm^{-3} as well (Fig. S2).

The IA concentration rises 1 order of magnitude, from 10^6 to 10^7 during 11–17 August 2019, when the wind direction changes abruptly (from 280–360° to 180–230°, marine air mass, Fig. 3). We found that during the marine-air-mass (180–230°, southeasterly over the Gulf of Finland and southwesterly over the northern Baltic Sea) influence over the study region, the average noontime maximum of SA and IA is on the order of 10^7 molec. cm^{-3} and that MSA is around 10^6 molec. cm^{-3} (Fig. 3). This is a concentration 1 order of magnitude higher than when the wind was from over the land (Fig. 3).

The highest concentration, 3×10^7 molec. cm^{-3}, of IA was observed when the wind was coming from the Baltic Sea sector, whereas the highest SA concentrations ($\sim 3 \times 10^7$ molec. cm^{-3}) were observed when the air mass traveled over the countries of Estonia and Russia, crossing the Gulf of Finland before entering the measurement site (land and sea region). The connection between the aerosol precursors and the wind direction can be observed in the cases where the wind direction changes rapidly. This highest IA concentration was recorded when the wind direction changes after 4 August to 180–230° (the Baltic Sea region). The change in wind direction was clearly reflected in a reversal of the concentration trends of SA and IA (Fig. 3). It was observed that the winds coming from 80–180° or 250–280° (land and sea region, Fig. 3) were SA-rich air masses. This comprises of the landmasses of south and northeastern Finland, northern Russia, part of the Gulf of Finland and Estonia, and the north to northwestern part of Finland including a part of the northernmost Gulf of Bothnia. The sectors 0–90° and 280–360° (land, Fig. 3) consist mostly of urban cities.

During the entire study period, when the air plume passed over the northern Baltic Sea region and the wind speed was high enough (> 4 m s^{-1}), high concentrations of IA were observed. While IA can be exclusively sourced from the marine and biogenic emissions (Mahajan et al., 2011; O'Dowd et al., 2002; Sipilä et al., 2016; Carpenter et al., 2021), SA could be biogenic and/or anthropogenic. Further, the temperatures prevailing during this period may have facilitated the DMS oxidation at a higher rate, which forms the source of biogenic SA and MSA. However, this is not a very simple equation, since this fractional yield of biogenic SA from DMS oxidation additionally also depends on the atmospheric NO_x ($NO + NO_2$) and HO_x ($OH + HO_2$) levels and on the scavenging of SO_2 by sea salt or cloud droplets (Hoffmann et al., 2016). The anthropogenic sources of SA for this site could also include vehicular or ship traffic, especially considering that there is a city road just 250 m and a harbor 6 km away from the measurement site. We explored the correlations of SA to a biogenic proxy, MSA, and the correlation with NO_x (anthropogenic proxy) to have a clear source apportionment of SA (Fig. 4). SO_2 could not be treated entirely as an anthropogenic proxy, as it can be sourced from DMS oxidation as well.

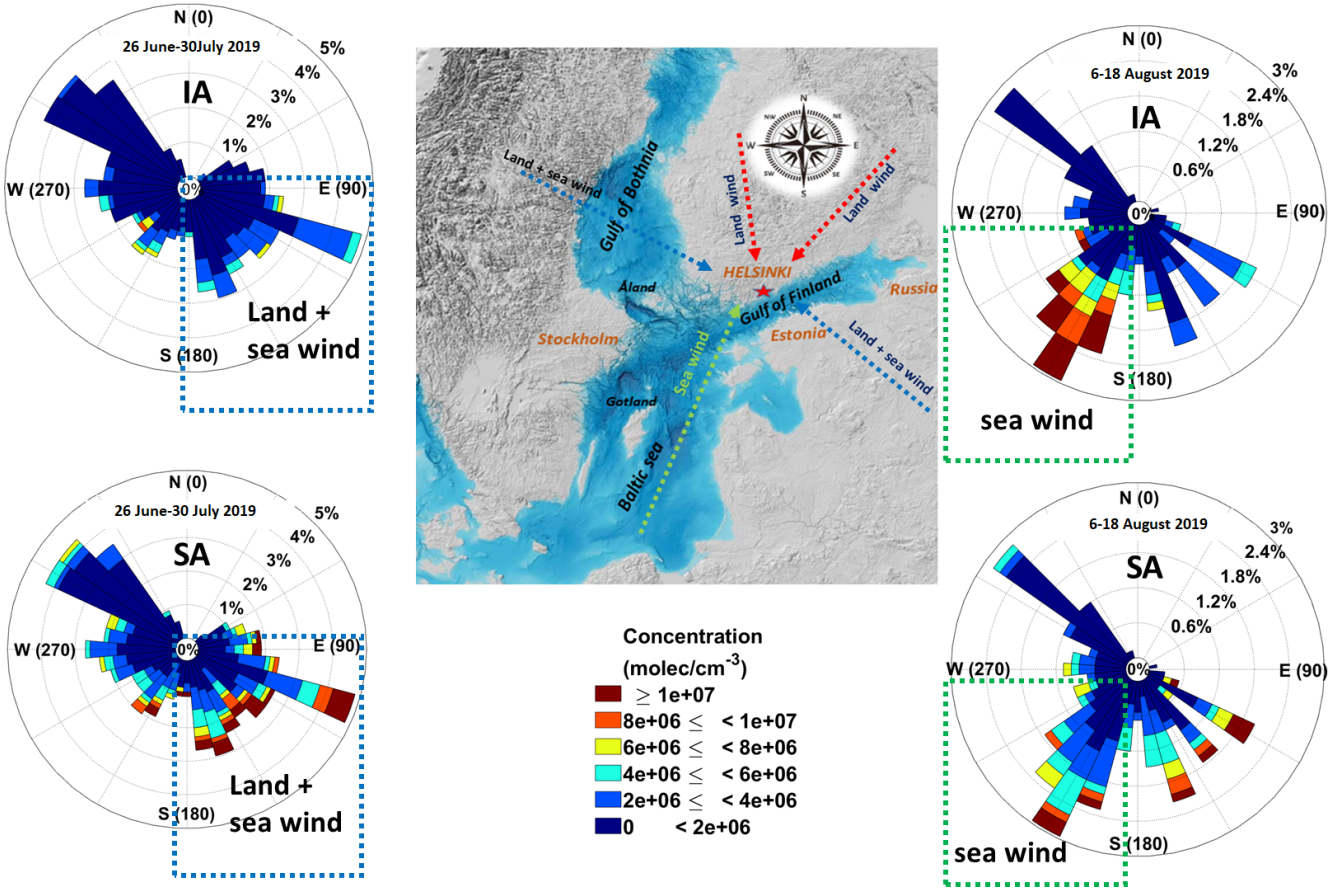

Figure 3. Wind roses showing the variability in the concentration of gases with wind direction during the study period. Percentages on the concentric circles denote the frequency of winds from different directions. The spokes are color-coded as per the concentration of the gas from the particular direction. The numbers in the parentheses within the wind roses refer to the wind direction in degrees.

The good correlations ($r_s > 0.6$, Fig. 4a and b) between SA and MSA during the study period (June–August) could suggest that they were sourced from a common biogenic source, the DMS emission from the cyanobacterial bloom. Good correlations of SA and MSA was also found in August ($r_s = 0.8$, Fig. 4b) when the air mass was mostly marine (and/or from the Finnish coastline, Fig. 3). Another observation was that SO_2 also shows some correlations with SA in both June–July and August study periods ($r_s = 0.4$, Fig. 4c and d) but not as significant as SA and MSA correlations. SO_2 can have different sources unlike MSA, which is mostly biogenic. However some emissions could be sourced from agriculture and other terrestrial sources (Bates et al., 1992); hence these observations could possibly indicate SA was more from biogenic sources than from other sources. But we cannot be very accurate in this estimation only by analyzing the correlation coefficients, since both MSA and SA can have a similar daily cycles due to the oxidation pathways.

Both SO_2 and MSA are the oxidation products of DMS (produced by phytoplankton, including some cyanobacteria), oxidized through an OH and NO_3 radical (Chen et al., 2000). Some of the previous chamber studies have confirmed that SO_2 is the major intermediate product formed from DMS oxidation (Sørensen et al., 1996; Berresheim et al., 1995). The SO_2 could be oxidized to SA (OH/O_2 oxidation) during the transport. Since our experimental site was surrounded by waterbodies and the summer season had enriched most of the freshwater and marine waters with abundant cyanobacterial blooms, this biogenic SA contribution to the study site has to be taken into account when analyzing the sources of SA. However, SO_2 can also be sourced from various anthropogenic activities and can be oxidized to SA. In Finland the major source of anthropogenic SO_2 is the public power industry, contributing almost 90 % to the total SO_2 emissions in Finland in the year 2019, while transport contributed to less than 1 % according to the emission inventory prepared by the Finnish Environment Institute (SYKE; Finnish air pollutant inventory, https://www.ymparisto.fi/en-US/Maps_and_statistics/Air_pollutant_emissions, last access: 20 October 2021). Further the maximum data points of high concentrations of SO_2 ($\sim 10^7$ molec. cm^{-3}) were not observed during the traffic hours in June–July–August (Fig. 4c and d),

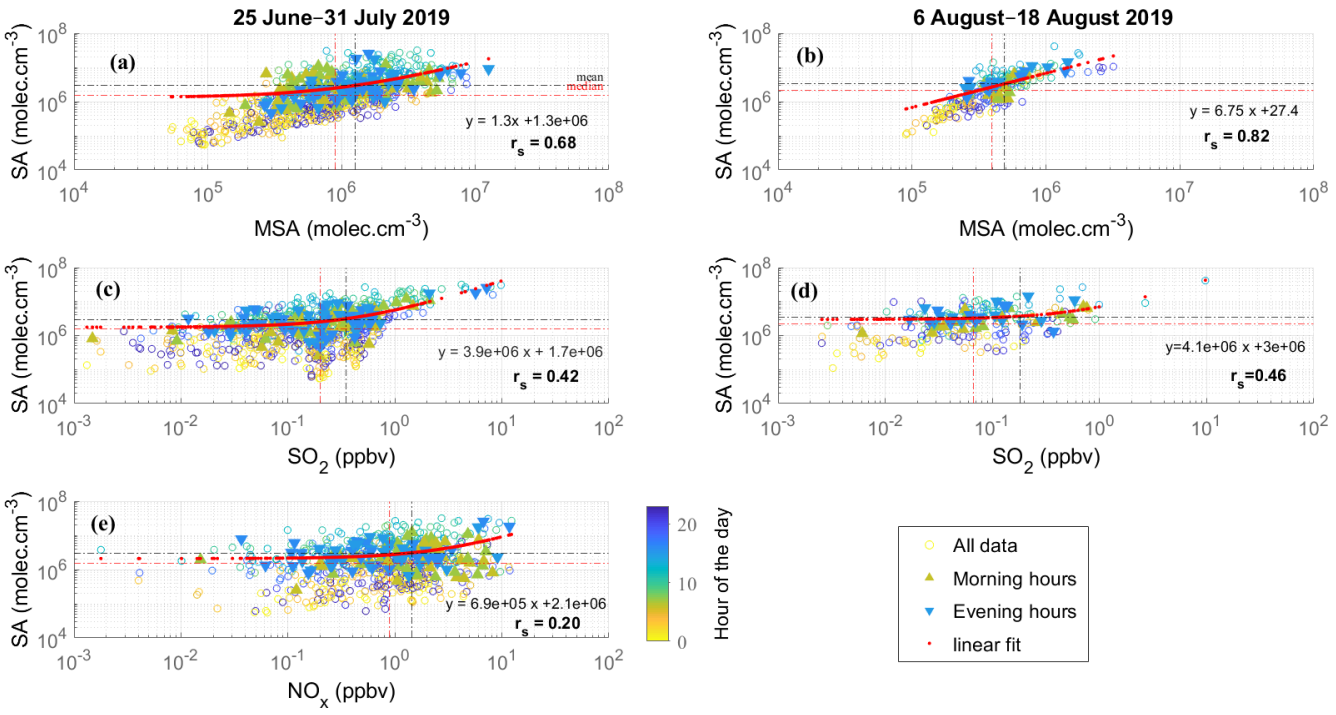

Figure 4. Correlation of SA with MSA **(a, b)**, SO_2 **(c, d)** and NO_x **(e)** for June–July. The black dashed lines for both axes represent the mean of the gas concentration; red dashed lines represent the median value of the gas concentrations; and red solid lines represent the linear fit. Spearman's coefficient (r_s) was used to test the correlation, at a significance level of 0.001. The circles represent data points at different hours of the day. The upward-pointing green triangles represent the morning rush hours (06:00–08:00), and the downward-pointing blue triangles represent the evening rush hours (15:00–17:00). The yellow hollow circles represent all data. NO_x data were unavailable for August.

another possible indication that biogenic sources could be contributing to the SO_2 concentrations and thus SA concentrations near the study site.

The emission inventory of Finland for the year 2019 indicated that sources of NO_x as NO_2 were mainly the power industries (41.5 %) and the transport sources (41 %) (https://www.ymparisto.fi/en-US/Maps_and_statistics/Air_pollutant_emissions, last access: 15 July 2020). These sources are indeed the most significant sources of NO_x globally (Meixner and Yang, 2006). NO_x, a definitive proxy to anthropogenic influence, shows a poor correlation with SA ($r_s = 0.28$, Fig. 4e) during June–July which could suggest an insignificant effect of traffic on the SA concentrations. Unfortunately, the NO_x data from August were unavailable due to instrument malfunction, so we cannot provide any correlations for this month.

The data presented in Fig. 3, where we observe high SA concentrations even when the air mass was marine and with the good correlations of SA and MSA (including of insignificant correlations of SA-NO_x) (Fig. 4), point towards a greater possibility of the influence of biogenic emissions on the concentrations of SA as compared to the anthropogenic emissions.

3.3 Types of nucleation events during the study

During 25 June–19 August 2019, we observe a number of NPF events characterized by a short appearance of ultrafine particles in the number size distribution lasting for less than 1 h. These so-called bursts/spikes appearing at small sizes (sub-3 nm) are indicative of local clustering processes in contrast to regional events, where it is possible to follow the growing particle mode for several hours (Dada et al., 2018; Dal Maso et al., 2005). Local clustering here means that the molecules could be transported from elsewhere, but the actual clustering could have taken place near the experimental site, indicated by a small bump of clusters (with absolutely little or no growth) as seen in the NAIS spectra. We do observe transported events (events with a growing particle mode but no small particles forming at the site) and non-event days, but they are not included in the analysis. This section discusses the occurrence of local and regional new particle formation events with the focus on (1) trace gas variability during the event days, (2) the evolution of differently sized particles during these events, (3) the impact of meteorological parameters and (4) the effect of cyanobacterial bloom on the events. The details of NPF events during the study period are described in Table 1.

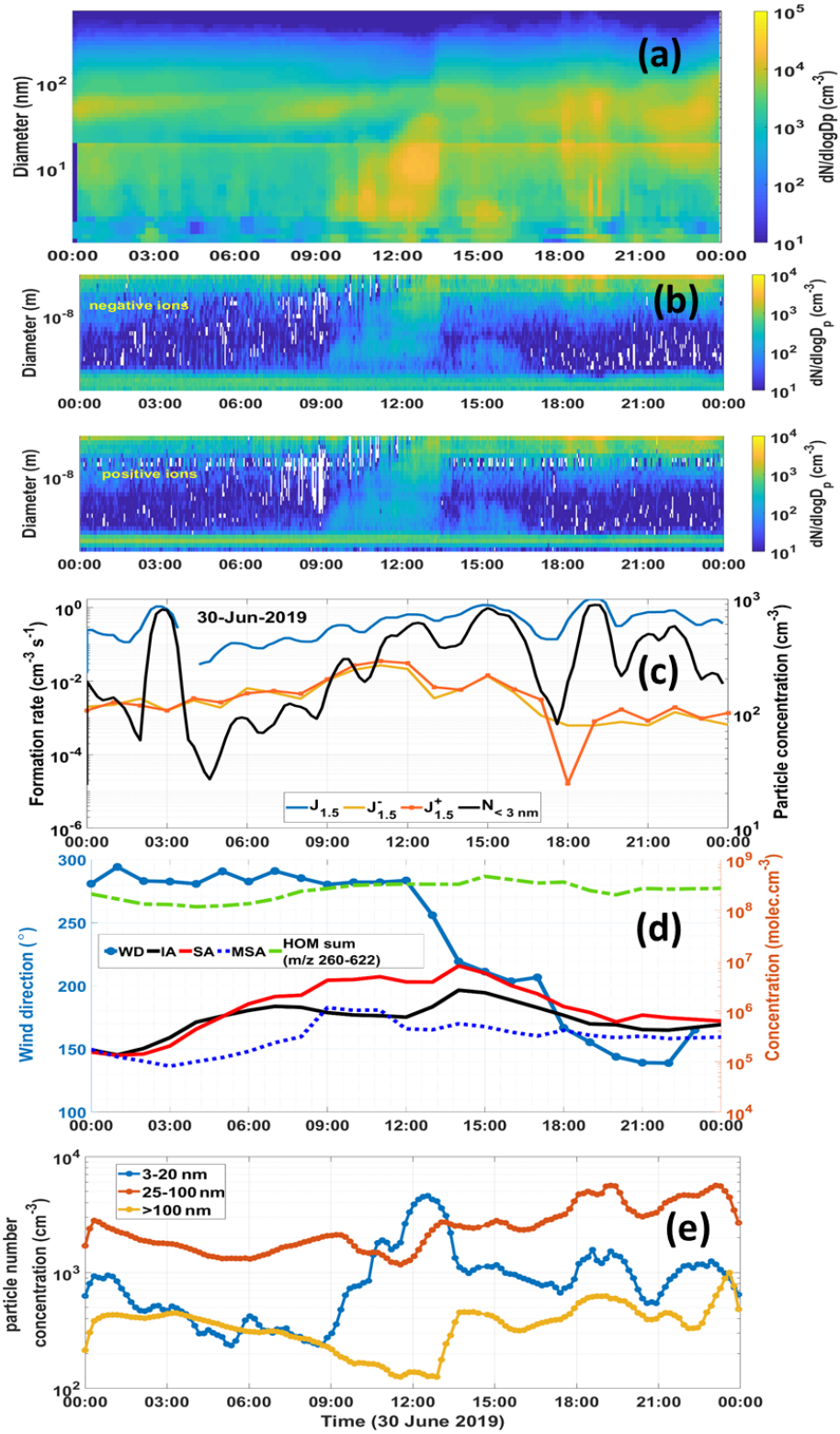

Figure 5. NPF event (regional and local events) on 30 June 2019. **(a)** Number size distribution of particles (data from the PSM, the NAIS and the DMPS; size range: sub-3–100 nm). **(b)** Charged-particle number size distribution (negative: upper, positive: lower) obtained from the NAIS. **(c)** Diurnal variation in formation rates ($J_{1.5}$) of 1.5 nm particles and ions ($J^{-}_{1.5}$ and $J^{+}_{1.5}$) on the left axis and particle number concentrations (1.5–3 nm) on the right axis. **(d)** Diurnal variation in HOMs, SA, IA and MSA with wind direction (WD). **(e)** The diurnal variation in particle concentration in nucleation (3–20 nm), Aitken (25–100 nm) and accumulation mode (> 100 nm) particles during the event (data from the DMPS).

Table 1. Timing and maximum concentration of SA, MSA and IA during local and burst/spike nucleation events during the study period.

Date	Type of event	Time of NPF (UTC+2)	SA (max) (molec. cm^{-3})	MSA (max) (molec. cm^{-3})	IA(max) (molec. cm^{-3})
30 June 2019	Regional/local	08:45–13:23, 14:00–16:30	7.9×10^6	5.6×10^5	2.3×10^6
30 July 2019	Regional/local	07:45–11:16	1.2×10^7	1.2×10^6	5.3×10^6
11 August 2019	Ion burst (spike)	13:40–14:32	1.0×10^7	1×10^6	3.2×10^7
14 August 2019	Ion burst (spike)	08:00–08:20	4.2×10^6	5.3×10^5	8.5×10^6
15 August 2019	Multiple ion bursts (spikes)	06:00, 08:58, 14:00–16:00	6.4×10^6 6.3×10^6 7.0×10^6	5.8×10^5 4.6×10^5 6.8×10^5	2.5×10^6 3.1×10^6 1.5×10^6

3.3.1 Nucleation: regional and local events

A regional NPF event was observed on 30 June 2019, which starts at 08:45 and ends at 13:23 (Fig. 5a). The negative ion clusters start to increase in concentration first at 08:45 (Fig. 5b), concurrent with the increase in concentration of the smallest particles (< 3 nm) from 10^2 to 10^3 cm^{-3} (Fig. 5c). Preceding the NPF event the SA concentrations were steadily increasing, and subsequently at 09:00, SA concentration doubles from 2×10^6 to 4×10^6 molec. cm^{-3} (Fig. 5d), while the particle formation rate at 1.5 nm ($J_{1.5}$) increased from 0.3 to 0.6 cm^{-3} s^{-1}. $J_{1.5}$ was much higher than either $J_{+1.5}$ or $J_{-1.5}$, thus indicating a neutral formation pathway rather than one that is ion mediated. Further we also observe a local clustering event at 15:00 with a simultaneous increase in the concentration of SA and HOMs along with an increase in the smallest particle concentration. This possibly indicates the role of SA and HOMs in the nucleation initiation. The high normalized signals of the DMA–SA cluster seen during the entire event (increasing from the start of the NPF event) possibly indicate that SA clusters initiate the event (Fig. S4a). DMA, including other main methylamines like mono- and trimethylamines (Bergman et al., 2015) in the global inventory (Schade and Crutzen, 1995), is contributed to through animal husbandry and other agricultural practices and biomass burning and by some contributions from marine and terrestrial sources. Although among these methylamine emissions, generally the trimethylamine dominates (Schade and Crutzen, 1995). Although no estimates of DMA measurements are available from the Helsinki region, the DMA in a boreal forest site in Finland has been estimated to be below ~ 150 ppqv (Sipilä et al., 2015), measured through an NO_3^- chemical ionization mass spectrometer. Their work also stated that DMA was unlikely to be playing an important role in the nucleation process observed at the site.

The increase in HOMs is also clearly observed during the event (Fig. S4b). Therefore we suggest that nucleation and the growth of particles were possibly due to SA organics, ensuring that particles reach the CCN and thus climate-relevant diameters. The work of Okuljar et al. (2021) also reports an increase in sub-3 nm particles with a simultaneous increase in SA concentration at the SMEAR III site, supporting our observations. However, the role of HOMs in nucleation initiation has not been explored at this site.

A clear increase in nucleation mode particles is seen during the event, starting at 08:45 (234 cm^{-3}) and reaching its maximum at 12:30 (4589 cm^{-3}). This increase in concentration of the nucleation mode particles was followed by the increase in concentration of Aitken mode and accumulation mode particles and continues for a couple of hours, indicating the growth of particles (Fig. 5e), possibly reaching CCN-relevant sizes. However, we also observe a drop in Aitken particles before NPF which also continues during NPF. We speculate it could be due to the change in wind direction (Väkevä et al., 2000) before NPF. The wind direction remains relatively constant throughout the NPF, so the low concentration of the Aitken mode continues. Wind direction changes abruptly at 12:00, and the Aitken mode particle concentrations increases soon after this change in wind direction (Fig. 5d). This shows that the particles must be in the process of growth mostly elsewhere, which is not evident in the changed air mass; however we still observe almost the same (or even slightly higher) precursor vapor concentrations, since the wind still passed over the bloom areas before entering our study site. After the change in local wind direction, the observed SA and IA slightly increase, and we still observe clustering (formation of small ions and particles) but no continuous growth typical of regional events. Figure 6a shows that > 40 % of the trajectories pass above the Swedish island of Gotland towards the southern part of the Bothnian Sea. The satellite data show that the bloom was present in the Bothnian Sea but not quite as dense as compared to the southern Baltic Sea (south of the island of Gotland) and the northern part of the Gulf of Finland (Fig. 6b). The majority of the trajectories did not pass over the dense cyanobacterial-bloom patch during this day (Fig. 6b). The

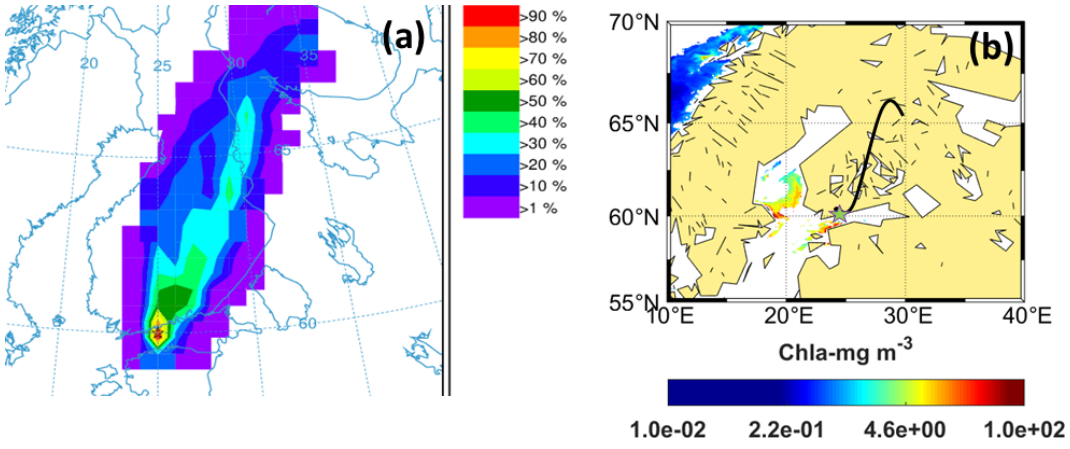

Figure 6. **(a)** Trajectory frequency plot (100 m a.g.l., arrival time of trajectories at the measurement site: 20:00) for 24 h back trajectory using GDAS (Global Data Assimilation System) meteorological input data (frequency grid resolution: 1.0° × 1.0°). **(b)** Chl *a* concentrations (GlobColour level 3). Black line shows the trajectory direction, and the star point denotes the measurement site.

calculated normalized residence time was higher over the neighboring cities of Helsinki (southwestern side) and parts of the Bothnian Sea during the event time (see Fig. S3). Thus the land-based anthropogenic activities and biogenic sources both can be contributing to SA concentrations for this event; here we cannot exactly quantify the source types for SA. However, the source of SA from the local sources such as vehicular traffic around our measurement site is small (as discussed above) but cannot be completely ignored (Olin et al., 2020).

The particle GR (7–25 nm) for this event was 16.5 nm h^{-1}, which is typical of a coastal site. Even when several condensing vapors participate in the growth process, growth rates typically do not exceed 20 nm h^{-1} (Kulmala et al., 2004). The GR for organics was calculated after subtracting the combined contribution of the GR of SA, IA and MSA from the measured particle GR (Fig. 7). The GR for organics should be treated as an estimation, since no separate GR calculations and assumptions were used. The calculated growth rates (GRs) show that SA can explain maximally 41 % of the growth of sub-3 nm particles, while IA and MSA can explain only < 1 % of the GR in this size range. The GR by SA in the bigger size fraction (7–25 nm) was only 0.51 nm h^{-1}, explaining only 3 % of the measured growth rate of particles. This means that vapors other than SA, IA and MSA were responsible for 96 % of the measured particle growth. These other vapors could include different organics, since they are known to contribute to the growth of particles (Kulmala et al., 1998, 2004; Riipinen et al., 2012; Zheng et al., 2020) and could better explain particle growth in the boreal forest (Ehn et al., 2014).

Another example of a regional event (neutral nucleation) probably driven by SA and organics was observed on 30 July 2019 (Fig. S5), which lasted for around 4 h. The trajectory frequency plots showed that most of the trajectories

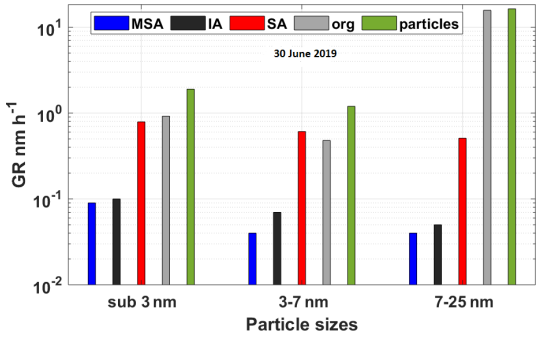

Figure 7. Particle growth rates calculated from the kinetic condensation of gases (data from CI–APi–TOF; org: organic) and the measured particle GRs (data from the NAIS) in different size classes on 30 June 2019.

were from the northern land areas (including urban cities and boreal forests) of Finland with the highest residence times over these land regions (Figs. S6 and S7). Since the precursor gases of biogenic origin, IA and MSA, do not show a significant concentration increase as compared to SA, at the start of the event, their contribution towards the initiation of the NPF event may not be as significant as SA. The greater residence times over the land areas clearly support the high SA and organic concentrations seen during the event, indicating an SA-driven event – with a possible contribution of HOMs (Fig. S7). In this case, SA explains 60 % of the growth of sub-3 nm particles compared to 41 % when the dominating trajectories passed over the Gulf of Finland (Fig. 5, 30 June 2019). Still, as for the previous case, a major fraction of the growth in the 3–7 nm range remains unexplained by the available acids (SA, IA and MSA) and is expected to be related to the contribution of organics. The GRs explained by SA in both the sub-3 nm (1.93 nm h^{-1}) and 3–7 nm (1.46 nm h^{-1}) size ranges are 58 %–59 % higher than on 30 June 2019 (0.79

and 0.61 nm h^{-1} for sub-3 and 3–7 nm, respectively), which could be explained by the increase in SA of 52 % on 30 July 2019. Thus, the events on 30 June and 30 July possibly occur via the nucleation of SA (possibly stabilized by bases, e.g., ammonia or amines), and the HOMs contribute to the growth of particles and possibly nucleation as well.

3.3.2 Nucleation: burst events

Case 1: biogenic IA nucleation – burst/spike events, 11 August 2019

Intense burst events are frequently observed at coastal sites accompanied with high concentrations of IA (O'Dowd et al., 2002; Rong et al., 2020; Sipilä et al., 2016). Two such bursts or spike events were observed on 11 August 2019 at 04:00 and 13:00 (Fig. 8a). Only the second spike event was observed in the NAIS size distribution with a higher intensity in the negative ion mode at 13:00 (Fig. 8b). During both these spike events we observe the formation of clusters (1.5 nm) and the formation rate ($J_{1.5}$) increases from 0.2 to 3.7 cm^{-3} s^{-1} during the event with a simultaneous significant increase in the sub-3 nm particle concentrations from ~ 100 to > 2000 cm^{-3} (Fig. 8c). $J^{+}_{1.5}$ and $J^{-}_{1.5}$ remain lower than the total formation rate, indicating this event to be a case of neutral nucleation. At the same time, IA shows an increase in concentration from 9×10^5 molec. cm^{-3} at 03:00 to 1×10^6 molec. cm^{-3} at 04:00. During this event the air masses changes from 160 to 140°; i.e., the direction of the air mass is changed to the Gulf of Finland. In the second burst (at 13:00), the IA concentration increases from 2×10^6 to 7×10^6 molec. cm^{-3} from 13:00 to 14:00 (Fig. 8d) with a slight change in wind direction from 151 to 166°. Most of these air masses are from the Gulf of Finland. SA concentration also increased but remained lower than IA during both the burst/spike events, indicating a possibility that iodine oxoacid formation initiates cluster formation (He et al., 2021b). We observe a growth of particles until 15:00 in the particle modes (NAIS data, Fig. 8b). However, the particles are seen reaching sizes up to size 100 nm (DMPS data, Fig. 8a). The organics almost remain constant within the range of 2–3 $\times 10^8$ molec. cm^{-3}. A further increase in IA concentration, 3×10^7 molec. cm^{-3} occurs at 15:00, and the concentration remains in the range of 10^7 molec. cm^{-3} for another 2 h (Fig. 8d). This was the highest observed IA concentration in the entire measurement period. A recent study by He et al. (2021b) indicates that IA concentrations above 1×10^7 molec. cm^{-3} leads to rapid new particle formation at +10 °C. At such concentrations the efficacy of iodine oxoacids to form new particles exceeds that of the H_2SO_4–NH_3 system at the same acid concentrations. Thus, the concentration of IA found in this event (2 times higher than SA during the start of the event), the high formation rates (> 1 cm^{-3} s^{-1}) and an unchanged concentration of SA during the event, as compared to the event on 30 June 2019, strongly suggest that it could be an IA-driven NPF event. In addition, a clear increase in the normalized signal of deprotonated IO_3^- with no significant increase in the DMA–SA cluster is noted at 13:00 (Fig. S8a). However, the HNO_3–IO_3^- cluster was the most abundant followed by the H_2O–IO_3^- cluster, indicating this event to be IA-driven nucleation. Further, between 14:00–15:00, when we observe the highest IA concentrations, a subsequent growth of particles is noted. We also observe an increasing number concentration of nucleation mode particles from 13:40 (~ 650 cm^{-3}) to 14:40 (~ 1800 cm^{-3}). After this 1 h of intense clustering, the Aitken mode particles also begin to increase in concentration from ~ 1300 to ~ 4800 cm^{-3} during 15:00–18:00 (Fig. 8e). The total particle concentration increased from ~ 2400 to ~ 6400 cm^{-3} within an hour during this burst event. We suggest that this burst event was possibly capable of producing particles big enough to act as CCN. Since it was an intense burst event with no proper horizontal growth (as seen in "banana" type events), we were not able to calculate the growth rate for this particular event. Therefore we are unable to quantify the contribution of IA towards the growth of particles reaching CCN sizes.

The global radiation and brightness parameter suggests that 11 August 2019 was overall cloudy until 12:30 (Fig. S9). The weather starts to change to clear-sky conditions after 13:00 when the brightness parameter increases from < 0.3 to ~ 0.7 (Fig. S9). The impact of the brightness parameter on NPF was also observed in a previous study (Dada et al., 2017). The clearing of the sky could explain the intense spike at 13:00 in the particle number size distribution as well as in the acid concentrations. For this particular case, we investigated further the source of such high IA concentrations, and we found that during this day, the maximum frequency of trajectories was observed over the southern Gulf of Finland (including the coastal waters of the island of Suomenlinna); however we do see the air masses coming in from the central Baltic Sea as well which was characterized by an intense bloom on this day (Fig. 9a). Interestingly, the cyanobacterial bloom was observed in three intense patches in the central Baltic Sea, southern Gulf of Finland (ship transect route between Helsinki and Tallinn) and Gulf of Riga (Fig. 9b). The sea level was also low, as it was observed to be 0.8–0.9 m in the coastal waters in around the measurement site (Suomenlinna and Gulf of Finland coastal measurement sites), supporting the exposure of the macroalgae to sunlight, which can be a good source of iodine precursors.

The residence time of the air masses coming from the Gulf of Finland and Baltic Sea was longer than the residence time of the air masses coming from the neighboring land areas (Fig. S10), clearly explaining the source of high IA observed during the event, which is through the blooms. Further, the air mass was completely marine at 15:00 when the highest IA is recorded, supporting the marine biogenic source of IA and its transport to the measurement site. The distance from the Gulf of Finland to the measurement site is approximately

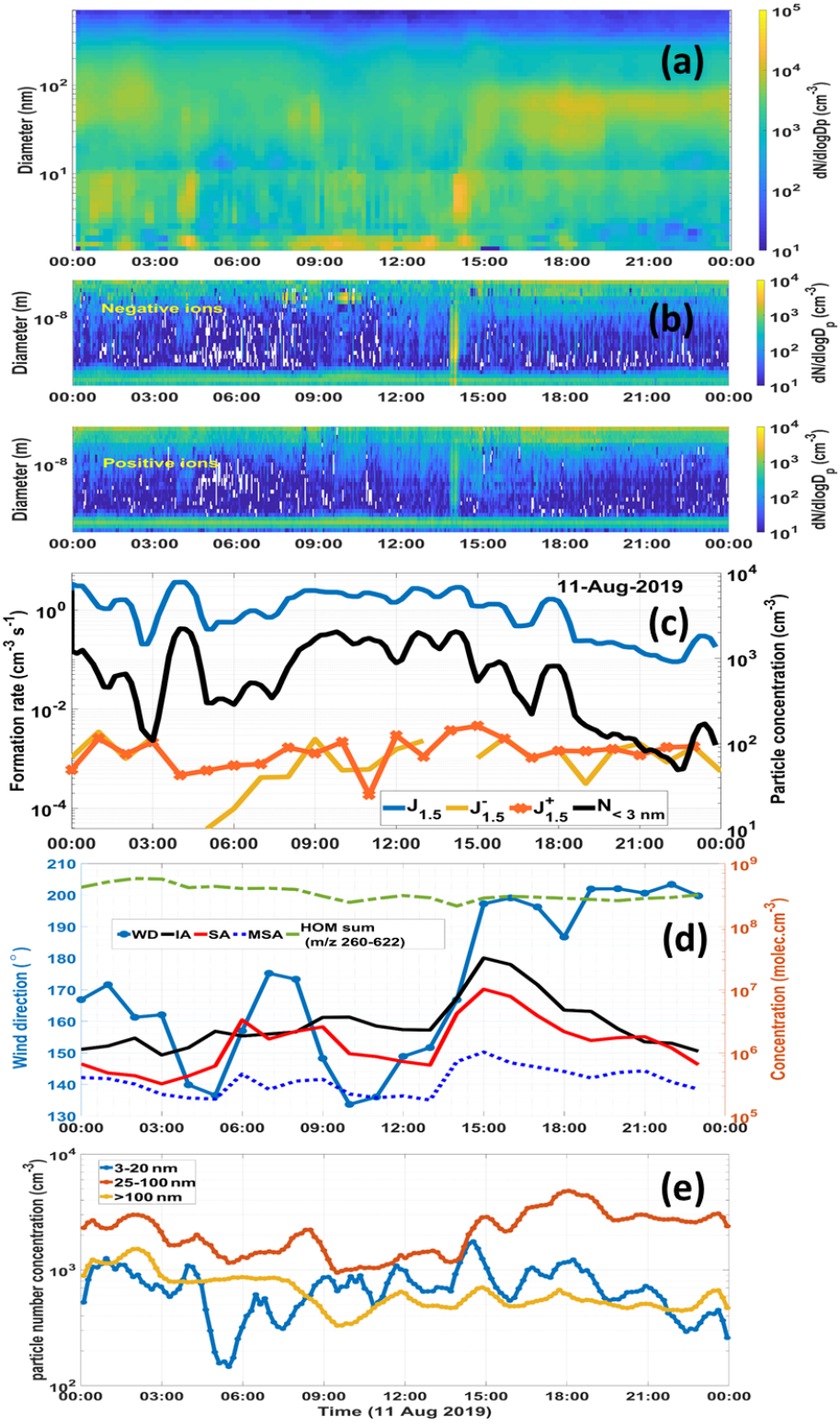

Figure 8. Burst event on 11 August 2019. **(a)** Number size distribution of particles (data from the PSM, the NAIS and the DMPS; size range: 1–100 nm). **(b)** Charged-particle number size distribution (negative: upper, positive: lower) obtained from the NAIS. **(c)** Diurnal variation in formation rates ($J_{1.5}$) of 1.5 nm particles and ions ($J^{-}_{1.5}$ and $J^{+}_{1.5}$) and total number concentrations of particles (< 3 nm, PSM). **(d)** Diurnal variation in HOMs, SA, IA and MSA with wind direction (WD). **(e)** The diurnal variation in particle concentration in nucleation (3–20 nm), Aitken (25–100 nm) and accumulation mode (> 100 nm) particles (DMPS data).

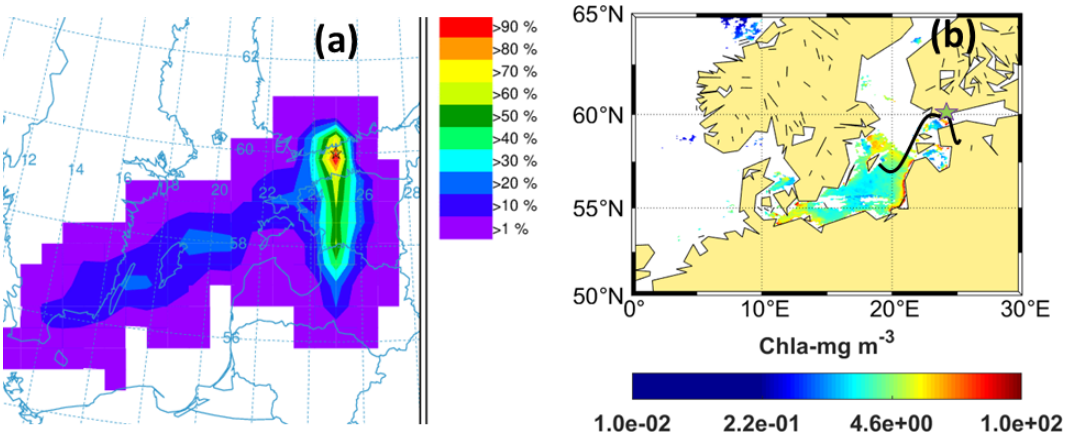

Figure 9. **(a)** Trajectory frequency plot (100 m a.g.l., arrival time of trajectories at the measurement site: 22:00) for 24 h back trajectory using GDAS meteorological input data (frequency grid resolution: 1.0° × 1.0°). **(b)** Chl *a* concentrations (GlobColour level 3). Black line shows the trajectory direction, and the star point denotes the measurement site.

5–10 km. With the wind speed of 5 m s^{-1} recorded during the event, it takes less than 1 h for the emission to transfer to our measurement site. By the time the air mass reached our measurement site from the emission source, a fraction of the emitted I_2 could have oxidized to IA. However, at this point we cannot differentiate between the sources of IA from neighboring coastal waters and the central Baltic Sea but can speculate that most of the IA observed could be sourced from the nearest coastal locations of the Gulf of Finland.

Another burst/spike event driven by IA occurred on 14 August 2019 (Fig. S11) when the IA concentration was found to be 8×10^6 molec. cm^{-3}, which was 2 times higher than SA concentration (4×10^6 molec. cm^{-3}). The event did not last more than 30 min. The precursor vapor concentration was not large enough for the event to continue or the particles to grow further. The meteorological conditions were very much similar to this event (11 August 2019). For this event also, the air mass was marine with maximum residence times over the Gulf of Finland and Baltic Sea regions. The vicinity of the emissions to the measurement site enabled the detection of these fast-forming clusters.

Case 2: biogenic SA nucleation – multiple bursts events

Another kind of event was observed on 15 August 2019 (Fig. 10a) where multiple particle bursts are observed and the particles grow to sizes > 50 nm.

The formation rates for the smallest clusters for both the polarities were the same ($J^+_{1.5}$ and $J^-_{1.5}$) (Fig. 10b and c). This was also the case for neutral nucleation as inferred from the relatively high (as compared to ions) $J_{1.5}$ (neutrals). On 15 August there was a sudden change in wind direction from the 180–215° (prominent wind direction during 11–14 August 2019) to 280°, and a series of bursts is triggered with the intense formation of clusters (< 3 nm) at each burst (Fig. 10d). The two most intense burst events were associated with an increase in SA from 2 to 6×10^6 molec. cm^{-3} at 06:00 and 5 to 7×10^6 molec. cm^{-3} at 14:00 (Fig. 10d). A third burst at 09:00 showed an increase in SA from 3 to 6×10^6 molec. cm^{-3}, and interestingly the concentration of IA_{max} increased to 3×10^6 molec. cm^{-3}. In all the three bursts a simultaneous increase in IA and MSA from 03:00 to 12:00 is observed, with the SA concentration being 2 to 3 times higher than IA and 4 to 5 times higher than MSA concentrations. The most intensive burst was at 14:00 (as compared to the burst at 06:00) when the SA was 3 times higher than IA. This burst was associated with a significant increase in Aitken mode particle concentration (from 1490 cm^{-3} at 14:00 to 4300 cm^{-3} at 15:00). The increase in accumulation particle concentration was seen just after 1 h from the start of the bursts for both events (06:00 and 14:00). However the increase in accumulation mode particle concentration for these two events was not very significant ($\sim$ 100 cm^{-3}), although particles reaching a size more than 80 nm (CCN relevant sizes) were observed. We saw DMA–SA clusters during the event (Fig. S12), which supports the observation that this an SA-driven NPF event.

During both these events (in fact, all the smaller burst events observed during this day), the trajectories were originating from Sweden (24 h prior to arrival). However, before entering the measurement site the trajectories passed over the southern part of the Gulf of Bothnia, and the trajectory frequency was > 70 % when the wind passed over the cyanobacterial-bloom region (Fig. 11a and b). To confirm our findings we checked a day where there was less intense bloom in the Gulf of Finland and northern Baltic Sea and the dominant air mass did not pass over the bloom patch in the Gulf of Finland (Fig. S13) before entering our experimental site. We did not observe an NPF event on this day, thereby suggesting that the air masses passing over the bloom patches

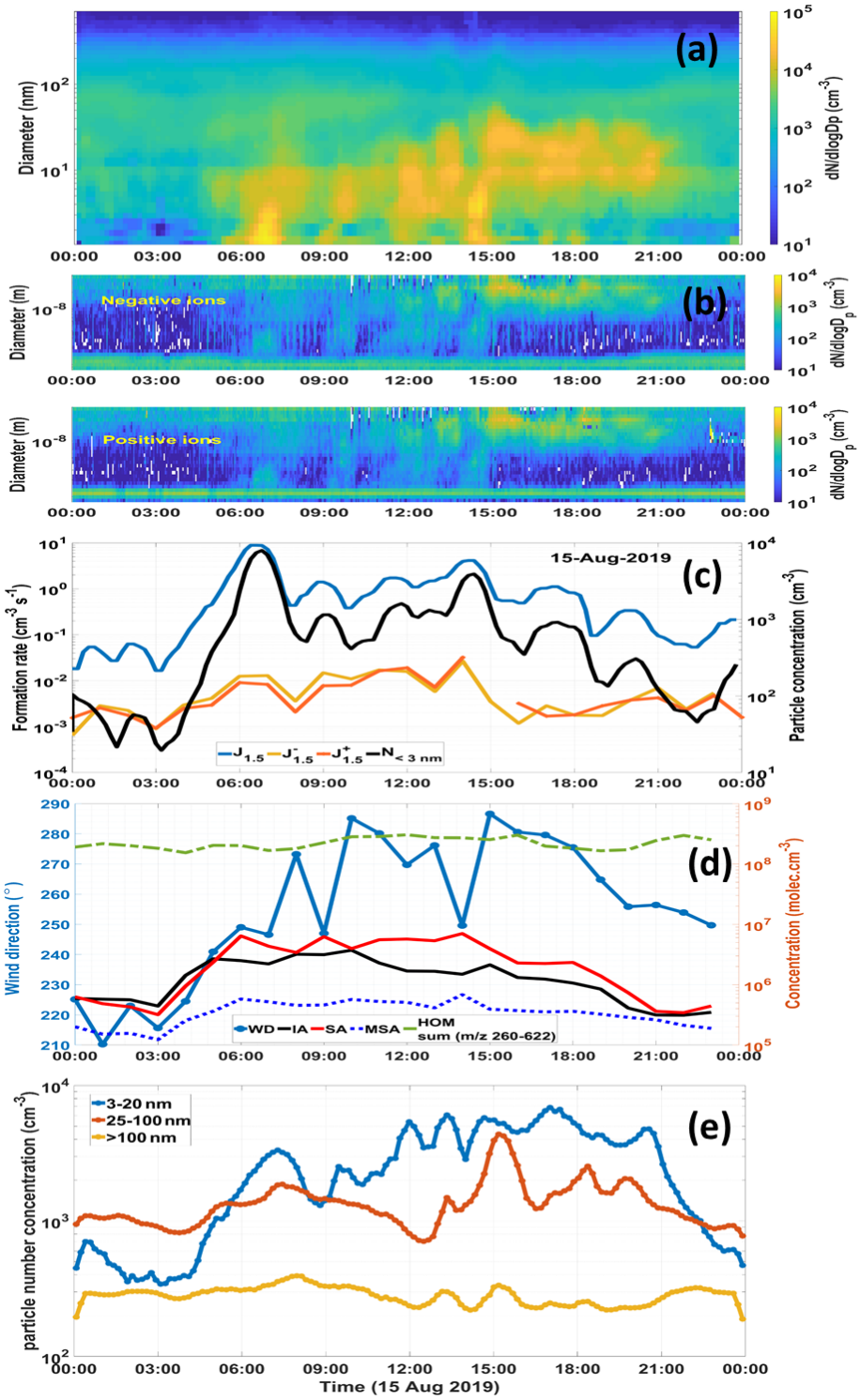

Figure 10. Multiple bursts/spikes on 15 August 2019. **(a)** Number size distribution of particles (data from the PSM, the NAIS and the DMPS; size range: 1–100 nm). **(b)** Charged-particle number size distribution (negative: upper, positive: lower) obtained from the NAIS. **(c)** Diurnal variation in formation rates ($J_{1.5}$) of 1.5 nm particles and ions ($J_{1.5}^{-}$ and $J_{1.5}^{+}$) and total number concentrations of particles (< 3 nm, PSM). **(d)** Diurnal variation in HOMs SA, IA and MSA with wind direction (WD). **(e)** The diurnal variation in particle concentration in nucleation (3–20 nm), Aitken (25–100 nm) and accumulation mode (> 100 nm) particles (DMPS data).

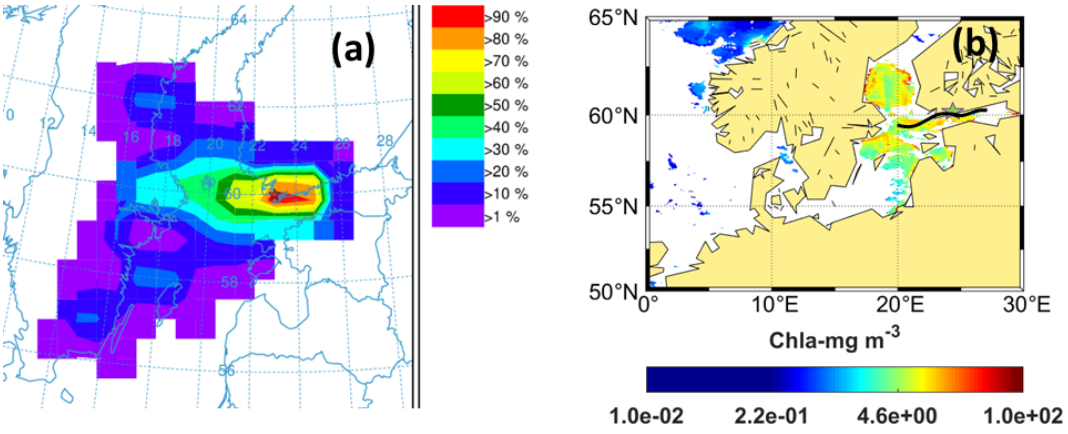

Figure 11. **(a)** Trajectory frequency plot (100 m a.g.l., arrival time of trajectories at the measurement site: 22:00) for 24 h back trajectory using GDAS meteorological input data (frequency grid resolution: 1.0° × 1.0°). **(b)** Chl *a* concentrations (GlobColour level 3). Black line shows the trajectory direction, and the star point denotes the measurement site.

before arriving at our study site were bringing in biogenic precursor vapors capable of initiating NPF events.

3.4 Possible contributions of biogenic emissions to precursor gaseous vapors

Assuming insignificant anthropogenic SA contribution as discussed in Sect. 3.2, we investigated the other possible sources of SA by evaluating the type of algae present in the waterbodies from where the air masses traveled during the events. The marine algae produce dimethylsulfoniopropionate (DMSP), which is capable of forming DMS, which subsequently oxidizes into SA and MSA. Very few cyanobacterial species are capable of producing DMSP (Karsten et al., 1996; Jonkers et al., 1998), and its concentration can vary considerably from one species to another (Keller et al., 1989). Moreover, blooms could be well mixed with other algal species (https://www.esa.int/ESA_Multimedia/Images/2019/12/Baltic_blooms, last access: 15 October 2019) which are capable of producing DMSP. A recent experiment identified *Aphanizomenon* as the only cyanobacteria-producing DMS (Steinke et al., 2018). The Gulf of Bothnia and Gulf of Riga are dominated by the genus *Aphanizomenon* (Kownacka et al., 2020). In addition, the Bothnian Sea and Gulf of Finland were found to be rich in the cyanobacterial genera of *Aphanizomenon*, *Nodularia* and *Dolichospermum* (Kownacka et al., 2020). As per the previous studies which were carried out as part of the Baltic-wide monitoring (Kownacka et al., 2020, and the references mentioned therein), bloom composition is fairly consistent for different regions and seasons from year to year, which makes it possible for us to make close estimations of the species present during our study in a particular region (from where the air mass travels and the residence time over a particular region).

A recent study also indicated that the abundance of DMS-producing cyanobacteria *Aphanizomenon* has increased in the Bothnian Sea due to decreasing salinity (Olofsson et al., 2020). Moreover, marine waters themselves are a large source of DMS (Kettle and Andreae, 2000), explaining the contribution of biogenic SA in the abovementioned burst events (15 August 2019). Hence to conclude, the marine regions surrounding the experimental site could be potential sources of biogenic SA. Moreover, high iodine emissions could be expected over the Baltic Sea region due to the presence of the macroalgal species which are well established and adapted there despite its low salinity (Kautsky and Kautsky, 2000; Schagerström et al., 2014) (note the high IA on 11 August 2019, event day). The rocky shorelines of the northern Baltic Sea provide ample habitat for several species of macroalgae, including *F. vesiculosus* (Kautsky and Kautsky, 2000; Torn et al., 2006). Previous studies have documented that certain macroalgae contain high levels of iodine (Ar Gall et al., 2004), of which the kelp *Laminaria digitata* stores the highest amount (Ar Gall et al., 2004; Küpper et al., 1998). A recent chamber experiment comparing different species of brown algae found that the emission rate of I_2 was higher in the case of *F. vesiculosus* when compared to other species like *L. digitata* (Huang et al., 2013). This could possibly explain the high IA concentration recorded by the CI–APi–TOF when the air mass was coming from the northern Baltic Sea (11 and 14 August 2019). The high production of macroalgal species is common along the extensive archipelago coastlines of the northern Baltic Sea, and particularly *F. vesiculosus* is likely to contribute with high emission rates, especially during peak production times when exposed to low sea levels and direct sunlight. However, partitioning the influence of macroalgae and microalgae requires further mechanistic studies. We suggest that marine and coastal regions surrounding the measurement site be capable of producing SA and IA during the bloom period, which can initiate NPF.

4 Conclusions

We studied the composition, concentrations and sources of precursor vapors forming aerosols in Helsinki, Finland, during the summer of 2019. The source of precursor gases responsible for new particle formation was assessed by analyzing the meteorological parameters and situation of cyanobacterial/algal bloom in the Baltic Sea. Our study recorded several regional, local and burst events, and we found that they were connected to elevated concentrations of SA and IA. The burst/spike events occurred simultaneously with high-intensity cyanobacterial/algal blooms in the Baltic Sea.

The study draws the following conclusions. (1) Constantly changing algal conditions in the Gulf of Bothnia, Gulf of Finland and Baltic Sea could be a significant source of the emission of iodine precursors and DMS. The gases produced by these emissions further oxidize in the atmosphere to form IA and SA, which can be detected by mass spectrometric methods. Interestingly, during marine-air-mass intrusion with higher residence time over the algal blooms, the gaseous precursors formed from the biological emissions possibly exceeded the gaseous precursors sourced from anthropogenic emissions at the measurement site. In fact, an overall higher impact of biogenic emissions was noted in this semi-urban site particularly during the end of July and mid-August when the bloom intensity decreases and the cyanobacteria/macroalgae start to decay and die (while being exposed to sunlight) and consequently produce more emissions (biogenic SA and IA). (2) Moreover, the meteorological conditions like wind direction and possibly wind speed were identified as the most important parameters influencing the precursor vapor concentration reaching the measurement site and thus determining if NPF occurred. Further we also infer that the wind direction played an important role in determining the particle concentrations at the study site. Our study reports that when the air mass traveled over the land with a higher residence time over the urban areas, it was enriched with SA and organics from proximal local sources leading to the occurrence of regional and local events (30 June and 30 July 2019). In contrast, when the air mass traveled over the waterbodies, with higher residence times over the cyanobacterial/algal blooms, the air mass was enriched with biogenic SA and/or IA initiating a burst/spike event at the measurement site (11, 14 and 15 August 2019). This observation is comparable to other coastal sites like Mace Head, although the NPF events are much stronger in Mace Head, since the measurement site is just at the coast with intensive low-tide–high-tide periods. (3) The formation rates of 1.5 nm particles and ions suggest that both IA-driven and SA-driven NPF events were neutral-nucleation events. (4) The type of phytoplankton species, intensity of the bloom and distance of the bloom from the experimental site is speculated to play an important role in determining the concentrations of precursor gases and thus influence the duration and type of NPF. The IA-driven nucleation occurred when the air mass traveled from over the Baltic Sea region, where the coasts are dominated by several species of macroalgae, including *F. vesiculosus*. The SA-rich burst events occurred when the air mass traveled over the Gulf of Bothnia, which was mainly dominated by the cyanobacteria species *Aphanizomenon*. (5) Burst/spike events, connected to high IA concentrations, likely led to the fast growth of particles potentially to CCN sizes. The role of stabilizing the IA clusters by SA and ammonia in a semi-urban coastal place needs to be further explored. The growth rate of particles was not fully explained by SA, IA and MSA alone – this applies especially for 3–7 nm or larger particles – indicating that organics might be playing a critical role in the growth of particles in this semi-urban location. We have significantly high ambient concentrations of HOMs in this study, although detailed descriptions are beyond the scope of this work.

The role of organics (HOMs) in the growth of particles is an active research question. Exploring the sources and characterizing them during a bloom period, when the emission of biogenic volatile organics increases with temperature, is crucial to understand the climate linkages of aerosol formation. In order to resolve these links, more quantitative studies are required which aim to understand the correlation between the quality and quantity of cyanobacterial blooms and the strength of emissions of aerosol precursor vapors. More systematic studies, partitioning the influence of pelagic cyanobacterial blooms and coastal macroalgae on new particle formation, would need to be undertaken.

Data availability. Mass spectrometer data for SA, IA, MSA and HOMs are available at https://doi.org/10.5281/zenodo.6426198 (Thakur et al., 2022). Neutral cluster and Air Ion Spectrometer data related to this article are available upon request to the corresponding author. The rest of the data are available for download from https://smear.avaa.csc.fi/download (Junninen et al., 2009).

Supplement. The supplement related to this article is available online at: https://doi.org/10.5194/acp-22-6365-2022-supplement.

Author contributions. RCT, TJ and MS designed the experiment. MS, LB, NS, YJT, TC, YJ, JL and ML were involved in the instrument installations and performed calibrations. RCT collected, processed, analyzed and interpreted the mass spectrometric data. TC, JS, JL, RCT and ML collected and processed the particle data. RCT, LD and KL interpreted the particle data. LD, LB, LQ and XCH preformed the calculations. MS, RCT, TJ and MK conceptualized the idea of connecting marine biology and atmospheric processes. AN edited and improved the paper's section on marine biology. CX carried out FLEXPART (FLEXible PARTicle dispersion model) analysis. MM contributed to the satellite data procurement and its interpretation. All authors contributed to and commented on the manuscript and interpreted the data.

Competing interests. At least one of the (co-)authors is a member of the editorial board of *Atmospheric Chemistry and Physics*. The peer-review process was guided by an independent editor, and the authors also have no other competing interests to declare.

Disclaimer. Publisher's note: Copernicus Publications remains neutral with regard to jurisdictional claims in published maps and institutional affiliations.

Acknowledgements. We thank the ACTRIS CiGAS-UHEL (Aerosol, Clouds and Trace Gases Research Infrastructure Centre for Trace Gases In Situ Measurements University of Helsinki) calibration center for providing the facility for CI–APi–TOF calibration and the INAR (Institute for Atmospheric and Earth System Research) technical staff for support during the entire experiment. We also acknowledge the Finnish Meteorological Institute for the provision of the wave height data in used this study from https://en.ilmatieteenlaitos.fi/wave-height (last access: 5 January 2022). We humbly acknowledge the useful discussion and data reference obtained from the Finnish Environment Institute. The authors gratefully acknowledge the NOAA Air Resources Laboratory (ARL) for the provision of the HYSPLIT transport and dispersion model and/or the READY website (Real-time Environmental Applications and Display sYstem; https://www.ready.noaa.gov, last access: 16 January 2022) used in this publication.

Financial support. This work was supported by the European Research Council (ERC) under the European Union's Horizon 2020 research and innovation program (GASPARCON, grant agreement no. 714621) and by the Academy of Finnish (grant agreement no. 334514). Funding was also provided by the Jane and Aatos Erkko Foundation; ERC ATM-GTP (Atmospheric Gas-to-Particle conversion); ACCC Flagship (Atmosphere and Climate Competence Center); and the Aerosols, Clouds and Trace Gases Research Infrastructure (ACTRIS).

Open-access funding was provided by the Helsinki University Library.

Review statement. This paper was edited by Drew Gentner and reviewed by two anonymous referees.

References

Aalto, P., Hämeri, K., Becker, E., Weber, R., Salm, J., Mäkelä, J. M., Hoell, C., O'Dowd, C. D., Hansson, H.-C., Väkevä, M., Koponen, I., Gintautas, B., and Kulmala, M.: Physical characterization of aerosol particles during nucleation events, Tellus B, 53, 344–358, 2001.

Allan, J. D., Williams, P. I., Najera, J., Whitehead, J. D., Flynn, M. J., Taylor, J. W., Liu, D., Darbyshire, E., Carpenter, L. J., Chance, R., Andrews, S. J., Hackenberg, S. C., and McFiggans, G.: Iodine observed in new particle formation events in the Arctic atmosphere during ACCACIA, Atmos. Chem. Phys., 15, 5599–5609, https://doi.org/10.5194/acp-15-5599-2015, 2015.

Almeida, J., Schobesberger, S., Kürten, A., Ortega, I. K., Kupiainen-Määttä, O., Praplan, A. P., Adamov, A., Amorim, A., Bianchi, F., Breitenlechner, M., David, A., Dommen, J., Donahue, N. M., Downard, A., Dunne, E., Duplissy, J., Ehrhart, S., Flagan, R. C., Franchin, A., Guida, R., Hakala, J., Hansel, A., Heinritzi, M., Henschel, H., Jokinen, T., Junninen, H., Kajos, M., Kangasluoma, J., Keskinen, H., Kupc, A., Kurtén, T., Kvashin, A. N., Laaksonen, A., Lehtipalo, K., Leiminger, M., Leppä, J., Loukonen, V., Makhmutov, V., Mathot, S., McGrath, M. J., Nieminen, T., Olenius, T., Onnela, A., Petäjä, T., Riccobono, F., Riipinen, I., Rissanen, M., Rondo, L., Ruuskanen, T., Santos, F. D., Sarnela, N., Schallhart, S., Schnitzhofer, R., Seinfeld, J. H., Simon, M., Sipilä, M., Stozhkov, Y., Stratmann, F., Tomé, A., Tröstl, J., Tsagkogeorgas, G., Vaattovaara, P., Viisanen, Y., Virtanen, A., Vrtala, A., Wagner, P. E., Weingartner, E., Wex, H., Williamson, C., Wimmer, D., Ye, P., Yli-Juuti, T., Carslaw, K. S., Kulmala, M., Curtius, J., Baltensperger, U., Worsnop, D. R., Vehkamäki, H., and Kirkby, J.: Molecular understanding of sulphuric acid-amine particle nucleation in the atmosphere, Nature, 502, 359–363, https://doi.org/10.1038/nature12663, 2013.

Ar Gall, E., Küpper, F. C., and Kloareg, B.: A survey of iodine content in Laminaria digitata, Bot. Mar., 47, 30–37, https://doi.org/10.1515/BOT.2004.004, 2004.

Artaxo, P., Rizzo, L. V., Brito, J. F., Barbosa, H. M. J., Arana, A., Sena, E. T., Cirino, G. G., Bastos, W., Martin, S. T., and Andreae, M. O.: Atmospheric aerosols in Amazonia and land use change: From natural biogenic to biomass burning conditions, Faraday Discuss., 165, 203–235, https://doi.org/10.1039/c3fd00052d, 2013.

Asmi, E., Kondratyev, V., Brus, D., Laurila, T., Lihavainen, H., Backman, J., Vakkari, V., Aurela, M., Hatakka, J., Viisanen, Y., Uttal, T., Ivakhov, V., and Makshtas, A.: Aerosol size distribution seasonal characteristics measured in Tiksi, Russian Arctic, Atmos. Chem. Phys., 16, 1271–1287, https://doi.org/10.5194/acp-16-1271-2016, 2016.

Attard, K. M., Rodil, I. F., Berg, P., Norkko, J., Norkko, A., and Glud, R. N.: Seasonal metabolism and carbon export potential of a key coastal habitat: The perennial canopy-forming macroalga Fucus vesiculosus, Limnol. Oceanogr., 64, 149–164, https://doi.org/10.1002/lno.11026, 2019.

Baalbaki, R., Pikridas, M., Jokinen, T., Laurila, T., Dada, L., Bezantakos, S., Ahonen, L., Neitola, K., Maisser, A., Bimenyimana, E., Christodoulou, A., Unga, F., Savvides, C., Lehtipalo, K., Kangasluoma, J., Biskos, G., Petäjä, T., Kerminen, V.-M., Sciare, J., and Kulmala, M.: Towards understanding the characteristics of new particle formation in the Eastern Mediterranean, At-

mos. Chem. Phys., 21, 9223–9251, https://doi.org/10.5194/acp-21-9223-2021, 2021.

Baccarini, A., Karlsson, L., Dommen, J., Duplessis, P., Vüllers, J., Brooks, I. M., Saiz-Lopez, A., Salter, M., Tjernström, M., Baltensperger, U., Zieger, P., and Schmale, J.: Frequent new particle formation over the high Arctic pack ice by enhanced iodine emissions, Nat. Commun., 11, 4924, https://doi.org/10.1038/s41467-020-18551-0, 2020.

Barnes, I., Hjorth, J., and Mihalopoulos, N.: Dimethyl sulfide and dimethyl sulfoxide and their oxidation in the atmosphere, Chem. Rev., 106, 940–975, 2006.

Bates, T. S., Lamb, B. K., Guenther, A., Dignon, J., and Stoiber, R. E.: Sulfur emissions to the atmosphere from natural sources, J. Atmos. Chem., 14, 315–337, https://doi.org/10.1007/BF00115242, 1992.

Beck, L. J., Sarnela, N., Junninen, H., Hoppe, C. J. M., Garmash, O., Bianchi, F., Riva, M., Rose, C., Peräkylä, O., Wimmer, D., Kausiala, O., Jokinen, T., Ahonen, L., Mikkilä, J., Hakala, J., He, X. C., Kontkanen, J., Wolf, K. K. E., Cappelletti, D., Mazzola, M., Traversi, R., Petroselli, C., Viola, A. P., Vitale, V., Lange, R., Massling, A., Nøjgaard, J. K., Krejci, R., Karlsson, L., Zieger, P., Jang, S., Lee, K., Vakkari, V., Lampilahti, J., Thakur, R. C., Leino, K., Kangasluoma, J., Duplissy, E. M., Siivola, E., Marbouti, M., Tham, Y. J., Saiz-Lopez, A., Petäjä, T., Ehn, M., Worsnop, D. R., Skov, H., Kulmala, M., Kerminen, V. M., and Sipilä, M.: Differing Mechanisms of New Particle Formation at Two Arctic Sites, Geophys. Res. Lett., 48, e2020GL091334, https://doi.org/10.1029/2020GL091334, 2021.

Benson, D. R., Young, L. H., Kameel, F. R., and Lee, S. H.: Laboratory-measured nucleation rates of sulfuric acid and water binary homogeneous nucleation from the $SO_2 + OH$ reaction, Geophys. Res. Lett., 35, 1–6, https://doi.org/10.1029/2008GL033387, 2008.

Bergman, T., Laaksonen, A., Korhonen, H., Malila, J., Dunne, E. M., Mielonen, T., Lehtinen, K. E. J., Kühn, T., Arola, A., and Kokkola, H.: Geographical and diurnal features of amine-enhanced boundary layer nucleation, J. Geophys. Res.-Atmos., 120, 9606–9624, https://doi.org/10.1002/2015JD023181, 2015.

Berresheim, H., Wine, P., and Davis, D.: Sulfur in the atmosphere, in: Composition Chemistry and climate of the Atmosphere, edited by: Singh, H. B., Van Nostrand Reinhold, New York, 251–307, ISBN 978-0-471-28514-4, 1995.

Berresheim, H., Elste, T., Plass-Dulmer, C., Eisele, F. L., and Tanner, D. J.: Chemical ionization mass spectrometer for long-term measurements of atmospheric OH and H_2SO_4, Int. J. Mass Spectrom., 202, 91–109, 2000.

Berresheim, H., Elste, T., Tremmel, H. G., Allen, A. G., Hansson, H. C., Rosman, K., Dal Maso, M., Mäkelä, J. M., Kulmala, M., and O'Dowd, C. D.: Gas-aerosol relationships of H_2SO_4, MSA, and OH: Observations in the coastal marine boundary layer at Mace Head, Ireland, J. Geophys. Res.-Atmos., 107, 1–12, https://doi.org/10.1029/2000JD000229, 2002.

Bianchi, F., Tröstl, J., Junninen, H., Frege, C., Henne, S., Hoyle, C. R., Molteni, U., Herrmann, E., Adamov, A., Bukowiecki, N., Chen, X., Duplissy, J., Gysel, M., Hutterli, M., Kangasluoma, J., Kontkanen, J., Kürten, A., Manninen, H. E., Münch, S., Peräkylä, O., Petäjä, T., Rondo, L., Williamson, C., Weingartner, E., Curtius, J., Worsnop, D. R., Kulmala, M., Dommen, J., and Baltensperger, U.: New particle formation in the free troposphere: A question of chemistry and timing, Science, 352, 1109–1112, https://doi.org/10.1126/science.aad5456, 2016.

Bianchi, F., Junninen, H., Bigi, A., Sinclair, V. A., Dada, L., Hoyle, C. R., Zha, Q., Yao, L., Ahonen, L. R., Bonasoni, P., Buenrostro Mazon, S., Hutterli, M., Laj, P., Lehtipalo, K., Kangasluoma, J., Kerminen, V. M., Kontkanen, J., Marinoni, A., Mirme, S., Molteni, U., Petäjä, T., Riva, M., Rose, C., Sellegri, K., Yan, C., Worsnop, D. R., Kulmala, M., Baltensperger, U., and Dommen, J.: Biogenic particles formed in the Himalaya as an important source of free tropospheric aerosols, Nat. Geosci., 14, 4–9, https://doi.org/10.1038/s41561-020-00661-5, 2020.

Bigg, E. K. and Turvey, D. E.: Sources of atmospheric particles over Australia, Atmos. Environ., 12, 1643–1655, https://doi.org/10.1016/0004-6981(78)90313-X, 1978.

Boy, M., Karl, T., Turnipseed, A., Mauldin, R. L., Kosciuch, E., Greenberg, J., Rathbone, J., Smith, J., Held, A., Barsanti, K., Wehner, B., Bauer, S., Wiedensohler, A., Bonn, B., Kulmala, M., and Guenther, A.: New particle formation in the Front Range of the Colorado Rocky Mountains, Atmos. Chem. Phys., 8, 1577–1590, https://doi.org/10.5194/acp-8-1577-2008, 2008.

Bryant, D. J., Dixon, W. J., Hopkins, J. R., Dunmore, R. E., Pereira, K. L., Shaw, M., Squires, F. A., Bannan, T. J., Mehra, A., Worrall, S. D., Bacak, A., Coe, H., Percival, C. J., Whalley, L. K., Heard, D. E., Slater, E. J., Ouyang, B., Cui, T., Surratt, J. D., Liu, D., Shi, Z., Harrison, R., Sun, Y., Xu, W., Lewis, A. C., Lee, J. D., Rickard, A. R., and Hamilton, J. F.: Strong anthropogenic control of secondary organic aerosol formation from isoprene in Beijing, Atmos. Chem. Phys., 20, 7531–7552, https://doi.org/10.5194/acp-20-7531-2020, 2020

Buenrostro Mazon, S., Kontkanen, J., Manninen, H. E., Nieminen, T., Kerminen, V. M., and Kulmala, M.: A long-term comparison of nighttime cluster events and daytime ion formation in a boreal forest, Boreal Environ. Res., 21, 242–261, 2016.

Cai, R. and Jiang, J.: A new balance formula to estimate new particle formation rate: reevaluating the effect of coagulation scavenging, Atmos. Chem. Phys., 17, 12659–12675, https://doi.org/10.5194/acp-17-12659-2017, 2017.

Carbone, M. S., Park Williams, A., Ambrose, A. R., Boot, C. M., Bradley, E. S., Dawson, T. E., Schaeffer, S. M., Schimel, J. P., and Still, C. J: Cloud shading and fog drip influence the metabolism of a coastal pine ecosystem, Glob. Change Biol., 19, 484–497, 2013.

Carpenter, L. J., Chance, R. J., Sherwen, T., Adams, T. J., Ball, S. M., Evans, M. J., Hepach, H., Hollis, L. D. J., Hughes, C., Jickells, T. D., Mahajan, A., Stevens, D. P., Tinel, L., and Wadley, M. R.: Marine iodine emissions in a changing world, P. Roy. Soc. A, 477, 20200824, https://doi.org/10.1098/rspa.2020.0824, 2021.

Chan, T., Cai, R., Ahonen, L. R., Liu, Y., Zhou, Y., Vanhanen, J., Dada, L., Chao, Y., Liu, Y., Wang, L., Kulmala, M., and Kangasluoma, J.: Assessment of particle size magnifier inversion methods to obtain the particle size distribution from atmospheric measurements, Atmos. Meas. Tech., 13, 4885–4898, https://doi.org/10.5194/amt-13-4885-2020, 2020.

Chen, D., Wang, W., Li, D., and Wang, W.: Atmospheric implication of synergy in methanesulfonic acid-base trimers: A theoretical investigation, RSC Adv., 10, 5173–5182, https://doi.org/10.1039/c9ra08760e, 2020.

Chen, H., Ezell, M. J., Arquero, K. D., Varner, M. E., Dawson, M. L., Gerber, R. B., and Finlayson-Pitts, B. J.: New parti-

cle formation and growth from methanesulfonic acid, trimethylamine and water, Phys. Chem. Chem. Phys., 17, 13699–13709, https://doi.org/10.1039/c5cp00838g, 2015.

Chen, H., Varner, M. E., Gerber, R. B., and Finlayson-Pitts, B. J.: Reactions of Methanesulfonic Acid with Amines and Ammonia as a Source of New Particles in Air, J. Phys. Chem. B, 120, 1526–1536, https://doi.org/10.1021/acs.jpcb.5b07433, 2016.

Chen, M., Titcombe, M., Jiang, J., Jen, C., Kuang, C., Fischer, M. L., Eisele, F. L., Siepmann, J. I., Hanson, D. R., Zhao, J., and McMurry, P. H.: Acid-base chemical reaction model for nucleation rates in the polluted atmospheric boundary layer, P. Natl. Acad. Sci. USA, 109, 18713–18718, https://doi.org/10.1073/pnas.1210285109, 2012.

Chen, Y. L., DeMott, P. J., Kreidenweis, S. M., Rogers, D. C., and Sherman, D. E.: Ice formation by sulfate and sulfuric acid aerosol particles under upper-tropospheric conditions, J. Atmos. Sci., 57, 3752–3766, 2000.

Croft, B., Martin, R. V., Leaitch, W. R., Tunved, P., Breider, T. J., D'Andrea, S. D., and Pierce, J. R.: Processes controlling the annual cycle of Arctic aerosol number and size distributions, Atmos. Chem. Phys., 16, 3665–3682, https://doi.org/10.5194/acp-16-3665-2016, 2016.

Dada, L., Paasonen, P., Nieminen, T., Buenrostro Mazon, S., Kontkanen, J., Peräkylä, O., Lehtipalo, K., Hussein, T., Petäjä, T., Kerminen, V.-M., Bäck, J., and Kulmala, M.: Long-term analysis of clear-sky new particle formation events and nonevents in Hyytiälä, Atmos. Chem. Phys., 17, 6227–6241, https://doi.org/10.5194/acp-17-6227-2017, 2017.

Dada, L., Chellapermal, R., Buenrostro Mazon, S., Paasonen, P., Lampilahti, J., Manninen, H. E., Junninen, H., Petäjä, T., Kerminen, V.-M., and Kulmala, M.: Refined classification and characterization of atmospheric new-particle formation events using air ions, Atmos. Chem. Phys., 18, 17883–17893, https://doi.org/10.5194/acp-18-17883-2018, 2018.

Dada, L., Ylivinkka, I., Baalbaki, R., Li, C., Guo, Y., Yan, C., Yao, L., Sarnela, N., Jokinen, T., Daellenbach, K. R., Yin, R., Deng, C., Chu, B., Nieminen, T., Wang, Y., Lin, Z., Thakur, R. C., Kontkanen, J., Stolzenburg, D., Sipilä, M., Hussein, T., Paasonen, P., Bianchi, F., Salma, I., Weidinger, T., Pikridas, M., Sciare, J., Jiang, J., Liu, Y., Petäjä, T., Kerminen, V.-M., and Kulmala, M.: Sources and sinks driving sulfuric acid concentrations in contrasting environments: implications on proxy calculations, Atmos. Chem. Phys., 20, 11747–11766, https://doi.org/10.5194/acp-20-11747-2020, 2020.

Dall'Osto, M., Geels, C., Beddows, D. C. S., Boertmann, D., Lange, R., Nøjgaard, J. K., Harrison, R. M., Simo, R., Skov, H., and Massling, A.: Regions of open water and melting sea ice drive new particle formation in North East Greenland, Sci. Rep., 8, 1–10, https://doi.org/10.1038/s41598-018-24426-8, 2018.

Dal Maso, M., Kulmala, M., Riipinen, I., Wagner, R., Hussein, T., Aalto, P. P., and Lehtinen, K. E. J.: Formation and growth of fresh atmospheric aerosols: Eight years of aerosol size distribution data from SMEAR II, Hyytiälä, Finland, Boreal Environ. Res., 10, 323–336, 2005.

Deng, C., Fu, Y., Dada, L., Yan, C., Cai, R., Yang, D., Zhou, Y., Yin, R., Lu, Y., Li, X., Qiao, X., Fan, X., Nie, W., Kontkanen, J., Kangasluoma, J., Chu, B., Ding, A., Kerminen, V. M., Paasonen, P., Worsnop, D. R., Bianchi, F., Liu, Y., Zheng, J., Wang, L., Kulmala, M., and Jiang, J.: Seasonal characteristics of new particle formation and growth in urban Beijing, Environ. Sci. Technol., 54, 8547–8557, https://doi.org/10.1021/acs.est.0c00808, 2020.

Du, W., Dada, L., Zhao, J., Chen, X., Daellenbach, K. R., Xie, C., Wang, W., He, Y., Cai, J., Yao, L., Zhang, Y., Wang, Q., Xu, W., Wang, Y., Tang, G., Cheng, X., Kokkonen, T. V., Zhou, W., Yan, C., Chu, B., Zha, Q., Hakala, S., Kurppa, M., Järvi, L., Liu, Y., Li, Z., Ge, M., Fu, P., Nie, W., Bianchi, F., Petäjä, T., Paasonen, P., Wang, Z., Worsnop, D. R., Kerminen, V. M., Kulmala, M., and Sun, Y.: A 3D study on the amplification of regional haze and particle growth by local emissions, npj Clim. Atmos. Sci., 4, 4, https://doi.org/10.1038/s41612-020-00156-5, 2021.

Duplissy, J., Merikanto, J., Franchin, A., Tsagkogeorgas, G., Kangasluoma, J., Wimmer, D., Vuollekoski, H., Schobesberger, S., Lehtipalo, K., Flagan, R. C., Brus, D., Donahue, N. M., Vehkamäki, H., Almeida, J., Amorim, A., Barmet, P., Bianchi, F., Breitenlechner, M., Dunne, E. M., Guida, R., Henschel, H., Junninen, H., Kirkby, J., Kürten, A., Kupc, A., Määttänen, A., Makhmutov, V., Mathot, S., Nieminen, T., Onnela, A., Praplan, A. P., Riccobono, F., Rondo, L., Steiner, G., Tome, A., Walther, H., Baltensperger, U., Carslaw, K. S.,Dommen, J., Hansel, A., Petäjä, T., Sipilä, M., Stratmann, F., Vrtala, A., Wagner, P. E., Worsnop, D. R., Curtius, J., and Kulmala, M.: Effect of ions on sulfuric acid-water binary particle formation: 1. Theory for kinetic- and nucleation-type particle formation and atmospheric implications, J. Geophys. Res.-Atmos., 121, 1736–1751, https://doi.org/10.1002/2015JD023538, 2016.

Ehn, M., Thornton, J. A., Kleist, E., Sipilä, M., Junninen, H., Pullinen, I., Springer, M., Rubach, F., Tillmann, R., Lee, B., Lopez-Hilfiker, F., Andres, S., Acir, I.-H. H., Rissanen, M., Jokinen, T., Schobesberger, S., Kangasluoma, J., Kontkanen, J., Nieminen, T., Kurtén, T., Nielsen, L. B., Jørgensen, S., Kjaergaard, H. G., Canagaratna, M., Maso, M. D., Berndt, T., Petäjä, T., Wahner, A., Kerminen, V.-M. M., Kulmala, M., Worsnop, D. R., Wildt, J., and Mentel, T. F.: A large source of low-volatility secondary organic aerosol, Nature, 506, 476–479, https://doi.org/10.1038/nature13032, 2014.

Eisele, F. L. and Tanner, D.: Measurement of the gas phase concentration of H_2SO_4 and Methane sulphonic acid and estimates of H_2SO_4 production and Loss in Atmosphere, J. Geophys. Res., 98, 9001–9010, 1993.

Eisele, F. L., Lovejoy, E. R., Kosciuch, E., Moore, K. F., Mauldin, I. L., Smith, J. N., McMurry, P. H., and Iida, K.: Negative atmospheric ions and their potential role in ion-induced nucleation, J. Geophys. Res.-Atmos., 111, D04305, https://doi.org/10.1029/2005JD006568, 2006.

Emery, N. C., D'Antonio, C. M., and Still, C. J.: Fog and live fuel moisture in coastal California shrublands Ecosphere, 9, e02167, https://doi.org/10.1002/ecs2.2167, 2018.

Fiedler, V., Dal Maso, M., Boy, M., Aufmhoff, H., Hoffmann, J., Schuck, T., Birmili, W., Hanke, M., Uecker, J., Arnold, F., and Kulmala, M.: The contribution of sulphuric acid to atmospheric particle formation and growth: a comparison between boundary layers in Northern and Central Europe, Atmos. Chem. Phys., 5, 1773–1785, https://doi.org/10.5194/acp-5-1773-2005, 2005.

Flanagan, R. J., Geever, M., and O'Dowd, C. D.: Direct measurements of new-particle fluxes in the coastal environment, Environ. Chem., 2, 256–259, https://doi.org/10.1071/EN05069, 2005.

Glasoe, W. A., Volz, K., Panta, B., Freshour, N., Bachman, R., Hanson, D. R., McMurry, P. H., and Jen, C.: Sulfuric acid nucleation:

An experimental study of the effect of seven bases, J. Geophys. Res., 120, 1933–1950, https://doi.org/10.1002/2014JD022730, 2015.

He, X. C., Iyer, S., Sipilä, M., Ylisirniö, A., Peltola, M., Kontkanen, J., Baalbaki, R., Simon, M., Kürten, A., Tham, Y. J., Pesonen, J., Ahonen, L. R., Amanatidis, S., Amorim, A., Baccarini, A., Beck, L., Bianchi, F., Brilke, S., Chen, D., Chiu, R., Curtius, J., Dada, L., Dias, A., Dommen, J., Donahue, N. M., Duplissy, J., El Haddad, I., Finkenzeller, H., Fischer, L., Heinritzi, M., Hofbauer, V., Kangasluoma, J., Kim, C., Koenig, T. K., Kubečka, J., Kvashnin, A., Lamkaddam, H., Lee, C. P., Leiminger, M., Li, Z., Makhmutov, V., Xiao, M., Marten, R., Nie, W., Onnela, A., Partoll, E., Petäjä, T., Salo, V. T., Schuchmann, S., Steiner, G., Stolzenburg, D., Stozhkov, Y., Tauber, C., Tomé, A., Väisänen, O., Vazquez-Pufleau, M., Volkamer, R., Wagner, A. C., Wang, M., Wang, Y., Wimmer, D., Winkler, P. M., Worsnop, D. R., Wu, Y., Yan, C., Ye, Q., Lehtinen, K., Nieminen, T., Manninen, H. E., Rissanen, M., Schobesberger, S., Lehtipalo, K., Baltensperger, U., Hansel, A., Kerminen, V. M., Flagan, R. C., Kirkby, J., Kurtén, T., and Kulmala, M.: Determination of the collision rate coefficient between charged iodic acid clusters and iodic acid using the appearance time method, Aerosol Sci. Tech., 55, 231–242, https://doi.org/10.1080/02786826.2020.1839013, 2021a.

He, X. C., Tham, Y. J., Dada, L., Wang, M., Finkenzeller, H., Stolzenburg, D., Iyer, S., Simon, M., Kürten, A., Shen, J., Rörup, B., Rissanen, M., Schobesberger, S., Baalbaki, R., Wang, D. S., Koenig, T. K., Jokinen, T., Sarnela, N., Beck, L. J., Almeida, J., Amanatidis, S., Amorim, A., Ataei, F., Baccarini, A., Bertozzi, B., Bianchi, F., Brilke, S., Caudillo, L., Chen, D., Chiu, R., Chu, B., Dias, A., Ding, A., Dommen, J., Duplissy, J., El Haddad, I., Carracedo, L. G., Granzin, M., Hansel, A., Heinritzi, M., Hofbauer, V., Junninen, H., Kangasluoma, J., Kemppainen, D., Kim, C., Kong, W., Krechmer, J. E., Kvashin, A., Laitinen, T., Lamkaddam, H., Lee, C. P., Lehtipalo, K., Leiminger, M., Li, Z., Makhmutov, V., Manninen, H. E., Marie, G., Marten, R., Mathot, S., Mauldin, R. L., Mentler, B., Möhler, O., Müller, T., Nie, W., Onnela, A., Petäjä, T., Pfeifer, J., Philippov, M., Ranjithkumar, A., Saiz-Lopez, A., Salma, I., Scholz, W., Schuchmann, S., Schulze, B., Steiner, G., Stozhkov, Y., Tauber, C., Tomé, A., Thakur, R. C., Väisänen, O., Vazquez-Pufleau, M., Wagner, A. C., Wang, Y., Weber, S. K., Winkler, P. M., Wu, Y., Xiao, M., Yan, C., Ye, Q., Ylisirniö, A., Zauner-Wieczorek, M., Zha, Q., Zhou, P., Flagan, R. C., Curtius, J., Baltensperger, U., Kulmala, M., Kerminen, V. M., Kurtén, T., et al.: Role of iodine oxoacids in atmospheric aerosol nucleation, Science, 371, 589–595, https://doi.org/10.1126/science.abe0298, 2021b.

Heikkinen, L., Äijälä, M., Riva, M., Luoma, K., Dällenbach, K., Aalto, J., Aalto, P., Aliaga, D., Aurela, M., Keskinen, H., Makkonen, U., Rantala, P., Kulmala, M., Petäjä, T., Worsnop, D., and Ehn, M.: Long-term sub-micrometer aerosol chemical composition in the boreal forest: inter- and intra-annual variability, Atmos. Chem. Phys., 20, 3151–3180, https://doi.org/10.5194/acp-20-3151-2020, 2020.

Hoffmann, E. H., Tilgner, A., Schrödner, R., Bräuer, P., Wolke, R., and Herrmann, H.: An advanced modeling study on the impacts and atmospheric implications of multiphase dimethyl sulfide chemistry, P. Natl. Acad. Sci. USA, 113, 11776–11781, https://doi.org/10.1073/pnas.1606320113, 2016.

Huang, R.-J., Seitz, K., Buxmann, J., Pöhler, D., Hornsby, K. E., Carpenter, L. J., Platt, U., and Hoffmann, T.: In situ measurements of molecular iodine in the marine boundary layer: the link to macroalgae and the implications for O_3, IO, OIO and NO_x, Atmos. Chem. Phys., 10, 4823–4833, https://doi.org/10.5194/acp-10-4823-2010, 2010.

Huang, R.-J., Thorenz, U. R., Kundel, M., Venables, D. S., Ceburnis, D., Ho, K. F., Chen, J., Vogel, A. L., Küpper, F. C., Smyth, P. P. A., Nitschke, U., Stengel, D. B., Berresheim, H., O'Dowd, C. D., and Hoffmann, T.: The seaweeds *Fucus vesiculosus* and *Ascophyllum nodosum* are significant contributors to coastal iodine emissions, Atmos. Chem. Phys., 13, 5255–5264, https://doi.org/10.5194/acp-13-5255-2013, 2013.

Humborg, C., Geibel, M. C., Sun, X., McCrackin, M., Mörth, C.-M., Stranne. C., Jakobsson, M., Gustafsson, B., Sokolov, A., Norkko, A., and Norkko, J.: High Emissions of Carbon Dioxide and Methane From the Coastal Baltic Sea at the End of a Summer Heat Wave. Front. Mar. Sci., 6, 493, https://doi.org/10.3389/fmars.2019.00493, 2019.

Iida, K., Stolzenburg, M. R., McMurry, P. H., and Smith, J. N.: Estimating nanoparticle growth rates from size-dependent charged fractions: Analysis of new particle formation events in Mexico City, J. Geophys. Res.-Atmos., 113, 1–15, https://doi.org/10.1029/2007JD009260, 2008.

Jang, E., Park, K.-T., Yoon, Y. J., Kim, T.-W., Hong, S.-B., Becagli, S., Traversi, R., Kim, J., and Gim, Y.: New particle formation events observed at the King Sejong Station, Antarctic Peninsula – Part 2: Link with the oceanic biological activities, Atmos. Chem. Phys., 19, 7595–7608, https://doi.org/10.5194/acp-19-7595-2019, 2019.

Jokinen, T., Sipilä, M., Junninen, H., Ehn, M., Lönn, G., Hakala, J., Petäjä, T., Mauldin III, R. L., Kulmala, M., and Worsnop, D. R.: Atmospheric sulphuric acid and neutral cluster measurements using CI-APi-TOF, Atmos. Chem. Phys., 12, 4117–4125, https://doi.org/10.5194/acp-12-4117-2012, 2012.

Jokinen, T., Kontkanen, J., Lehtipalo, K., Manninen, H. E., Aalto, J., Porcar-Castell, A., Garmash, O., Nieminen, T., Ehn, M., Kangasluoma, J., Junninen, H., Levula, J., Duplissy, J., Ahonen, L. R., Rantala, P., Heikkinen, L., Yan, C., Sipilä, M., Worsnop, D. R., Bäck, J., Petäjä, T., Kerminen, V.-M., and Kulmala, M.: Solar eclipse demonstrating the importance of photochemistry in new particle formation, Sci. Rep., 7, 632, https://doi.org/10.1038/srep45707, 2017.

Jokinen, T., Sipilä, M., Kontkanen, J., Vakkari, V., Tisler, P., Duplissy, E. M., Junninen, H., Kangasluoma, J., Manninen, H. E., Petäjä, T., Kulmala, M., Worsnop, D. R., Kirkby, J., Virkkula, A., and Kerminen, V. M.: Ion-induced sulfuric acid–ammonia nucleation drives particle formation in coastal Antarctica, Sci. Adv., 4, 1–7, https://doi.org/10.1126/sciadv.aat9744, 2018.

Jonkers, H. M., Bruin, S. D., and Gemerden, H. V.: Turnover of dimethylsulfoniopropionate (DMSP) by the purple sulfur bacterium Thiocapsa roseopersicina M11: ecological implications, FEMS Microbiol. Ecol., 27, 281–290, https://doi.org/10.1111/j.1574-6941.1998.tb00544.x, 1998.

Junninen, H., Lauri, A., Keronen, P., Aalto, P., Hiltunen, V., Hari, P., and Kulmala, M.: Smart-SMEAR: online data exploration and visualization tool for SMEAR stations, Boreal Environ. Res., 14, 447–457, 2009.

Junninen, H., Ehn, M., Petäjä, T., Luosujärvi, L., Kotiaho, T., Kostiainen, R., Rohner, U., Gonin, M., Fuhrer, K., Kulmala, M., and Worsnop, D. R.: A high-resolution mass spectrometer to measure atmospheric ion composition, Atmos. Meas. Tech., 3, 1039–1053, https://doi.org/10.5194/amt-3-1039-2010, 2010.

Kahru, M. and Elmgren, R.: Multidecadal time series of satellite-detected accumulations of cyanobacteria in the Baltic Sea, Biogeosciences, 11, 3619–3633, https://doi.org/10.5194/bg-11-3619-2014, 2014.

Karsten, U., Kuck, K., Vogt, C., and Kirst, G. O.: Dimethylsulphoniopropioante production in phototrophic organisms and its physiological function as a cryoprotectant, in: Biological and Environmental Chemstry of DMSP and Related Sulphonium Compounds, edited by: Kiene, R. P., Visscher, P. T., Keller, M. D., and Kirst, G. O., Plenum Press, New York, NY, 143–153, ISBN 978-1-4613-0377-0, 1996.

Kautsky, L. and Kautsky, N.: The Baltic Sea, including Bothnian Sea and Bothnian Bay, in: Seas at the millennium: an environmental evaluation: 1. Regional chapters: Europe, The Americas and West Africa, edited by: Sheppard, C. R. C., Elsevier Science, 121–133, 2000.

Keller, M. D., Bellows, W. K., and Guillard, R. R. L.: Dimethyl Sulfide Production in Marine Phytoplankton, in: Biogenic Sulfur in the Environment, edited by: Saltzman, E. S. and Cooper, W. J., American Chemical Society, 11, 167–182, https://doi.org/10.1021/bk-1989-0393.ch011, 1989.

Kettle, A. J. and Andreae, M. O.: Flux of dimethylsulfide from the oceans: A comparison of updated data sets and flux models, J. Geophys. Res.-Atmos., 105, 26793–26808, https://doi.org/10.1029/2000JD900252, 2000.

Kirkby, J., Curtius, J., Almeida, J., Dunne, E., Duplissy, J., Ehrhart, S., Franchin, A., Gagné, S., Ickes, L., Kürten, A., Kupc, A., Metzger, A., Riccobono, F., Rondo, L., Schobesberger, S., Tsagkogeorgas, G., Wimmer, D., Amorim, A., Bianchi, F., Breitenlechner, M., David, A., Dommen, J., Downard, A., Ehn, M., Flagan, R. C., Haider, S., Hansel, A., Hauser, D., Jud, W., Junninen, H., Kreissl, F., Kvashin, A., Laaksonen, A., Lehtipalo, K., Lima, J., Lovejoy, E. R., Makhmutov, V., Mathot, S., Mikkilä, J., Minginette, P., Mogo, S., Nieminen, T., Onnela, A., Pereira, P., Petäjä, T., Schnitzhofer, R., Seinfeld, J. H., Sipilä, M., Stozhkov, Y., Stratmann, F., Tomé, A., Vanhanen, J., Viisanen, Y., Vrtala, A., Wagner, P. E., Walther, H., Weingartner, E., Wex, H., Winkler, P. M., Carslaw, K. S., Worsnop, D. R., Baltensperger, U., and Kulmala, M.: Role of sulphuric acid, ammonia and galactic cosmic rays in atmospheric aerosol nucleation, Nature, 476, 429–435, https://doi.org/10.1038/nature10343, 2011.

Kirkby, J., Duplissy, J., Sengupta, K., Frege, C., Gordon, H., Williamson, C., Heinritzi, M., Simon, M., Yan, C., Almeida, J., Trostl, J., Nieminen, T., Ortega, I. K., Wagner, R., Adamov, A., Amorim, A., Bernhammer, A. K., Bianchi, F., Breitenlechner, M., Brilke, S., Chen, X., Craven, J., Dias, A., Ehrhart, S., Flagan, R. C., Franchin, A., Fuchs, C., Guida, R., Hakala, J., Hoyle, C. R., Jokinen, T., Junninen, H., Kangasluoma, J., Kim, J., Krapf, M., Kurten, A., Laaksonen, A., Lehtipalo, K., Makhmutov, V., Mathot, S., Molteni, U., Onnela, A., Perakyla, O., Piel, F., Petaja, T., Praplan, A. P., Pringle, K., Rap, A., Richards, N. A. D., Riipinen, I., Rissanen, M. P., Rondo, L., Sarnela, N., Schobesberger, S., Scott, C. E., Seinfeld, J. H., Sipila, M., Steiner, G., Stozhkov, Y., Stratmann, F., Tomé, A., Virtanen, A., Vogel, A. L., Wagner, A. C., Wagner, P. E., Weingartner, E., Wimmer, D., Winkler, P. M., Ye, P., Zhang, X., Hansel, A., Dommen, J., Donahue, N. M., Worsnop, D. R., Baltensperger, U., Kulmala, M., Carslaw, K. S., and Curtius, J.: Ion-induced nucleation of pure biogenic particles, Nature, 533, 521–526, https://doi.org/10.1038/nature17953, 2016.

Klawonn, I., Nahar, N., Walve, J., Andersson, B., Olofsson, M., Svedén, J. B., Littmann, S., Whitehouse, M. J., Kuypers, M. M., and Ploug, H.: Cell-specific nitrogen- and carbon-fixation of cyanobacteria in a temperate marine system (Baltic Sea), Environ. Microbiol., 12, 4596–4609, https://doi.org/10.1111/1462-2920.13557, 2016.

Knutson, T., Zhang, R., and Horowitz, L.: Prospects for a prolonged slowdown in global warming in the early 21st century, Nat. Commun., 7, 13676, https://doi.org/10.1038/ncomms13676, 2016.

Kownacka, J., Busch, S., Göbel, J., Gromisz, S., Hällfors, H., Höglander, H., Huseby, S., Jaanus, A., Jakobsen, H. H., Johansen, M., Johansson, M., Jurgensone, I., Liebeke, N., Kraśniewski, W., Kremp, A., Lehtinen, S., Olenina, I., Weber, M., and Wasmund, N.: Cyanobacteria biomass 1990–2019, HELCOM Baltic Sea Environment Fact Sheets, Eutrophication – HELCOM [date viewed: 24 January 2021], 2020.

Kuang, C., McMurry, P. H., McCormick, A. V., and Eisele, F. L.: Dependence of nucleation rates on sulfuric acid vapor concentration in diverse atmospheric locations, J. Geophys. Res., 113, D10209, https://doi.org/10.1029/2007JD009253, 2008.

Kulmala, M., Toivonen, A., Mäkelä, J. M., and Laaksonen, A.: Analysis of the growth of nucleation mode particles observed in Boreal forest, Tellus B, 50, 449–462, https://doi.org/10.3402/tellusb.v50i5.16229, 1998.

Kulmala, M., Pirjola, L., and Mäkelä, J. M.: Stable sulphate clusters as a source of new atmospheric particles, Nature 404, 66–69, https://doi.org/10.1038/35003550, 2000.

Kulmala, M., Laakso, L., Lehtinen, K. E. J., Riipinen, I., Dal Maso, M., Anttila, T., Kerminen, V.-M., Hõrrak, U., Vana, M., and Tammet, H.: Initial steps of aerosol growth, Atmos. Chem. Phys., 4, 2553–2560, https://doi.org/10.5194/acp-4-2553-2004, 2004.

Kulmala, M., Kontkanen, J., Junninen, H., Lehtipalo, K., Manninen, H. E., Nieminen, T., Petäjä, T., Sipilä, M., Schobesberger, S., Rantala, P., Franchin, A., Jokinen, T., Järvinen, E., Äijälä, M., Kangasluoma, J., Hakala, J., Aalto, P. P., Paasonen, P., Mikkilä, J., Vanhanen, J., Aalto, J., Hakola, H., Makkonen, U., Ruuskanen, T., Mauldin, R. L., Duplissy, J., Vehkamäki, H., Bäck, J., Kortelainen, A., Riipinen, I., Kurtén, T., Johnston, M. V., Smith, J. N., Ehn, M., Mentel, T. F., Lehtinen, K. E. J., Laaksonen, A., Kerminen, V. M., and Worsnop, D. R.: Direct observations of atmospheric aerosol nucleation, Science, 339, 943–946, https://doi.org/10.1126/science.1227385, 2013.

Kulmala, M., Petäjä, T., Kerminen, V. M., Kujansuu, J., Ruuskanen, T., Ding, A., Nie, W., Hu, M., Wang, Z., Wu, Z., Wang, L., and Worsnop, D. R.: On secondary new particle formation in China, Front. Environ. Sci. En., 10, 1–10, https://doi.org/10.1007/s11783-016-0850-1, 2016.

Kulmala, M., Kerminen, V. M., Petäjä, T., Ding, A. J., and Wang, L.: Atmospheric gas-to-particle conversion: Why NPF events are observed in megacities?, Faraday Discuss., 200, 271–288, https://doi.org/10.1039/c6fd00257a, 2017.

Kulmala, M., Kokkonen, T. V., Pekkanen, J., Paatero, S., Petäjä, T., Kerminen, V.-M., and Ding, A.: Opinion: Gigacity – a source

of problems or the new way to sustainable development, Atmos. Chem. Phys., 21, 8313–8322, https://doi.org/10.5194/acp-21-8313-2021, 2021.

Kuosa, H., Fleming-Lehtinen, V., Lehtinen, S., Lehtiniemi, M., Nygård, H., Raateoja, M., Raitaniemi, J., Tuimala, J., Uusitalo, L., and Suikkanen, S.: A retrospective view of the development of the Gulf of Bothnia ecosystem, J. Marine Syst., 167, 78–92, https://doi.org/10.1016/j.jmarsys.2016.11.020, 2017.

Küpper, F. C., Schweigert, N., Ar Gall, E., Legendre, J. M., Vilter, H., and Kloareg, B.: Iodine uptake in Laminariales involves extracellular, haloperoxidase-mediated oxidation of iodide, Planta, 207, 163–171, https://doi.org/10.1007/s004250050469, 1998.

Kürten, A., Rondo, L., Ehrhart, S., and Curtius, J.: Calibration of a chemical ionization mass spectrometer for the measurement of gaseous sulfuric acid, J. Phys. Chem. A, 116, 6375–6386, https://doi.org/10.1021/jp212123n, 2012.

Kürten, A., Jokinen, T., Simon, M., Sipilä, M., Sarnela, N., Junninen, H., Adamov, A., Almeida, J., Amorim, A., Bianchi, F., Breitenlechner, M., Dommen, J., Donahue, N. M., Duplissy, J., Ehrhart, S., Flagan, R. C., Franchin, A., Hakala, J., Hansel, A., Heinritzi, M., Hutterli, M., Kangasluoma, J., Kirkby, J., Laaksonen, A., Lehtipalo, K., Leiminger, M., Makhmutov, V., Mathot, S., Onnela, A., Petäjä, T., Praplan, A. P., Riccobono, F., Rissanen, M. P., Rondo, L., Schobesberger, S., Seinfeld, J. H., Steiner, G., Tomé, A., Tröstl, J., Winkler, P. M., Williamson, C., Wimmer, D., Ye, P., Baltensperger, U., Carslaw, K. S., Kulmala, M., Worsnop, D. R., and Curtius, J.: Neutral molecular cluster formation of sulfuric acid-dimethylamine observed in real time under atmospheric conditions, P. Natl. Acad. Sci. USA, 111, 15019–15024, https://doi.org/10.1073/pnas.1404853111, 2014.

Kürten, A., Münch, S., Rondo, L., Bianchi, F., Duplissy, J., Jokinen, T., Junninen, H., Sarnela, N., Schobesberger, S., Simon, M., Sipilä, M., Almeida, J., Amorim, A., Dommen, J., Donahue, N. M., Dunne, E. M., Flagan, R. C., Franchin, A., Kirkby, J., Kupc, A., Makhmutov, V., Petäjä, T., Praplan, A. P., Riccobono, F., Steiner, G., Tomé, A., Tsagkogeorgas, G., Wagner, P. E., Wimmer, D., Baltensperger, U., Kulmala, M., Worsnop, D. R., and Curtius, J.: Thermodynamics of the formation of sulfuric acid dimers in the binary (H_2SO_4–H_2O) and ternary (H_2SO_4–H_2O–NH_3) system, Atmos. Chem. Phys., 15, 10701–10721, https://doi.org/10.5194/acp-15-10701-2015, 2015.

Kürten, A., Bianchi, F., Almeida, J., Kupiainen-Määttä, O., Dunne, E. M., Duplissy, J., Williamson, C., Barmet, P., Breitenlechner, M., Dommen, J., Donahue, N. M., Flagan, R. C., Franchin, A., Gordon, H., Hakala, J., Hansel, A., Heinritzi, M., Ickes, L., Jokinen, T., Kangasluoma, J., Kim, J., Kirkby, J., Kupc, A., Lehtipalo, K., Leiminger, M., Makhmutov, V., Onnela, A., Ortega, I. K., Petäjä, T., Praplan, A. P., Riccobono, F., Rissanen, M. P., Rondo, L., Schnitzhofer, R., Schobesberger, S., Smith, J. N., Steiner, G., Stozhkov, Y., Tomé, A., Tröstl, J., Tsagkogeorgas, G., Wagner, P. E., Wimmer, D., Ye, P., Baltensperger, U., Carslaw, K., Kulmala, M., and Curtius, J.: Experimental particle formation rates spanning tropospheric sulfuric acid and ammonia abundances, ion production rates, and temperatures, J. Geophys. Res., 121, 12377–12400, https://doi.org/10.1002/2015JD023908, 2016.

Kurtén, T., Petäjä, T., Smith, J., Ortega, I. K., Sipilä, M., Junninen, H., Ehn, M., Vehkamäki, H., Mauldin, L., Worsnop, D. R., and Kulmala, M.: The effect of H_2SO_4 – amine clustering on chemical ionization mass spectrometry (CIMS) measurements of gas-phase sulfuric acid, Atmos. Chem. Phys., 11, 3007–3019, https://doi.org/10.5194/acp-11-3007-2011, 2011.

Kyrö, E.-M., Väänänen, R., Kerminen, V.-M., Virkkula, A., Petäjä, T., Asmi, A., Dal Maso, M., Nieminen, T., Juhola, S., Shcherbinin, A., Riipinen, I., Lehtipalo, K., Keronen, P., Aalto, P. P., Hari, P., and Kulmala, M.: Trends in new particle formation in eastern Lapland, Finland: effect of decreasing sulfur emissions from Kola Peninsula, Atmos. Chem. Phys., 14, 4383–4396, https://doi.org/10.5194/acp-14-4383-2014, 2014.

Lawson, D. M., Clemesha, R. E. S., Vanderplank, S., Gershunov, A., and Cayan, D.: Impacts and influences of coastal low clouds and fog on biodiversity in San Diego California's Fourth Climate Change Assessment CCCA4-EXT-2018-010 69–89, https://www.energy.ca.gov/sites/default/files/2019-12/Biodiversity_CCCA4-EXT-2018-010_ada_0.pdf (last access: 24 August 2021), 2018.

Lehtipalo, K., Leppä, J., Kontkanen, J., Kangasluoma, J., Franchin, A., Wimmer, D., Schobesberger, S., Junninen, H., Petäjä, T., Sipilä, M., Mikkilä, J., Vanhanen, J., Worsnop, D. R., and Kulmala, M.: Methods for determining particle size distribution and growth rates between 1 and 3 nm using the Particle Size Magnifier, Boreal Environ. Res., 19, 215–236, 2014.

Lehtipalo, K., Yan, C., Dada, L., Bianchi, F., Xiao, M., Wagner, R., Stolzenburg, D., Ahonen, L. R., Amorim, A., Baccarini, A., Bauer, P. S., Baumgartner, B., Bergen, A., Bernhammer, A. K., Breitenlechner, M., Brilke, S., Buchholz, A., Mazon, S. B., Chen, D., Chen, X., Dias, A., Dommen, J., Draper, D. C., Duplissy, J., Ehn, M., Finkenzeller, H., Fischer, L., Frege, C., Fuchs, C., Garmash, O., Gordon, H., Hakala, J., He, X., Heikkinen, L., Heinritzi, M., Helm, J. C., Hofbauer, V., Hoyle, C. R., Jokinen, T., Kangasluoma, J., Kerminen, V.-M., Kim, C., Kirkby, J., Kontkanen, J., Kürten, A., Lawler, M. J., Mai, H., Mathot, S., Mauldin III, R. L., Molteni, U., Nichman, L., Nie, W., Nieminen, T., Ojdanic, A., Onnela, A., Passananti, M., Petäjä, T., Piel, F., Pospisilova, V., Quéléver, L. L. J., Rissanen, M. P., Rose, C., Sarnela, N., Schallhart, S., Schuchmann, S., Sengupta, K., Simon, M., Sipilä, M., Tauber, C., Tomé, A., Tröstl, J., Väisänen, O., Vogel, A. L., Volkamer, R., Wagner, A. C., Wang, M., Weitz, L., Wimmer, D., Ye, P., Ylisirniö, A., Zha, Q., Carslaw, K. S., Curtius, J., Donahue, N. M., Flagan, R. C., Hansel, A., Riipinen, I., Virtanen, A., Winkler, P. M., Baltensperger, U., Kulmala, M., and Worsnop, D. R.: Multicomponent new particle formation from sulfuric acid, ammonia, and 979 biogenic vapors, Sci. Adv., 4, eaau536, https://doi.org/10.1126/sciadv.aau5363, 2018.

Leino, K., Nieminen, T., Manninen, H. E., Petäjä, T., Kerminen, V. M., and Kulmala, M.: Intermediate ions as a strong indicator of new particle formation bursts in boreal forest, Boreal Environ. Res., 21, 274–286, 2016.

Mahajan, A. S., Oetjen, H., Saiz-Lopez, A., Lee, J. D., McFiggans, G. B., and Plane, J. M. C.: Reactive iodine species in a semi-polluted environment, Geophys. Res. Lett., 36, 6–11, https://doi.org/10.1029/2009GL038018, 2009.

Mahajan, A. S., Sorribas, M., Gómez Martín, J. C., MacDonald, S. M., Gil, M., Plane, J. M. C., and Saiz-Lopez, A.: Concurrent observations of atomic iodine, molecular iodine and ultrafine particles in a coastal environment, Atmos. Chem. Phys., 11, 2545–2555, https://doi.org/10.5194/acp-11-2545-2011, 2011.

Manninen, H. E., Nieminen, T., Asmi, E., Gagné, S., Häkkinen, S., Lehtipalo, K., Aalto, P., Vana, M., Mirme, A., Mirme, S., Hõrrak, U., Plass-Dülmer, C., Stange, G., Kiss, G., Hoffer, A., Törő, N., Moerman, M., Henzing, B., de Leeuw, G., Brinkenberg, M., Kouvarakis, G. N., Bougiatioti, A., Mihalopoulos, N., O'Dowd, C., Ceburnis, D., Arneth, A., Svenningsson, B., Swietlicki, E., Tarozzi, L., Decesari, S., Facchini, M. C., Birmili, W., Sonntag, A., Wiedensohler, A., Boulon, J., Sellegri, K., Laj, P., Gysel, M., Bukowiecki, N., Weingartner, E., Wehrle, G., Laaksonen, A., Hamed, A., Joutsensaari, J., Petäjä, T., Kerminen, V.-M., and Kulmala, M.: EUCAARI ion spectrometer measurements at 12 European sites – analysis of new particle formation events, Atmos. Chem. Phys., 10, 7907–7927, https://doi.org/10.5194/acp-10-7907-2010, 2010.

Mauldin III, R., Eisele, F., Tanner, D., Kosciuch, E., Shetter, R., Lefer, B., Hall, S., Nowak, J., Buhr, M., Chen, G., Wang, P., and Davis, D.: Measurements of OH, H_2SO_4, and MSA at the South Pole during ISCAT, Geophys. Res. Lett., 28, 3629–3632, https://doi.org/10.1016/j.atmosenv.2004.06.031, 20011.

McFiggans, G., Coe, H., Burgess, R., Allan, J., Cubison, M., Alfarra, M. R., Saunders, R., Saiz-Lopez, A., Plane, J. M. C., Wevill, D., Carpenter, L., Rickard, A. R., and Monks, P. S.: Direct evidence for coastal iodine particles from Laminaria macroalgae – linkage to emissions of molecular iodine, Atmos. Chem. Phys., 4, 701–713, https://doi.org/10.5194/acp-4-701-2004, 2004.

McFiggans, G., Bale, C. S. E., Ball, S. M., Beames, J. M., Bloss, W. J., Carpenter, L. J., Dorsey, J., Dunk, R., Flynn, M. J., Furneaux, K. L., Gallagher, M. W., Heard, D. E., Hollingsworth, A. M., Hornsby, K., Ingham, T., Jones, C. E., Jones, R. L., Kramer, L. J., Langridge, J. M., Leblanc, C., LeCrane, J.-P., Lee, J. D., Leigh, R. J., Longley, I., Mahajan, A. S., Monks, P. S., Oetjen, H., Orr-Ewing, A. J., Plane, J. M. C., Potin, P., Shillings, A. J. L., Thomas, F., von Glasow, R., Wada, R., Whalley, L. K., and Whitehead, J. D.: Iodine-mediated coastal particle formation: an overview of the Reactive Halogens in the Marine Boundary Layer (RHaMBLe) Roscoff coastal study, Atmos. Chem. Phys., 10, 2975–2999, https://doi.org/10.5194/acp-10-2975-2010, 2010.

Meixner, F. X. and Yang, W. X.: Biogenic emissions of nitric oxide and nitrous oxide from arid and semi-arid land, in: Dryland Ecohydrology, edited by: D'Odorico, P. and Porporato, A., Springer, Dordrecht, https://doi.org/10.1007/1-4020-4260-4_14, 2006.

Mirme, S. and Mirme, A.: The mathematical principles and design of the NAIS – a spectrometer for the measurement of cluster ion and nanometer aerosol size distributions, Atmos. Meas. Tech., 6, 1061–1071, https://doi.org/10.5194/amt-6-1061-2013, 2013.

Nieminen, T., Asmi, A., Aalto, P. P., Keronen, P., Petäjä, T., Kulmala, M., Kerminen, V. M., Nieminen, T., and Dal Maso, M.: Trends in atmospheric new-particle formation: 16 years of observations in a boreal-forest environment, Boreal Environ. Res., 19, 191–214, 2014.

O'Dowd, C. D., Lowe, J. A., Smith, M. H., Davison, B., Hewitt, C. N., and Harrison, R. M.: Biogenic sulphur emissions and inferred non-sea-salt-sulphate particularly during Events of new particle formation were Instrumentation and Cruise Summary, Atlantic, J. Geophys. Res.-Atmos., 102, 12839-12854, https://doi.org/10.1029/96JD02749,1997

O'Dowd, C. D., Jimenez, J. L., Bahreini, R., Flagan, R. C., Seinfeld, J. H., Hämerl, K., Pirjola, L., Kulmala, M., and Hoffmann, T.: Marine aerosol formation from biogenic iodine emissions, Nature, 417, 632–636, https://doi.org/10.1038/nature00775, 2002.

Okuljar, M., Kuuluvainen, H., Kontkanen, J., Garmash, O., Olin, M., Niemi, J. V., Timonen, H., Kangasluoma, J., Tham, Y. J., Baalbaki, R., Sipilä, M., Salo, L., Lintusaari, H., Portin, H., Teinilä, K., Aurela, M., Dal Maso, M., Rönkkö, T., Petäjä, T., and Paasonen, P.: Measurement report: The influence of traffic and new particle formation on the size distribution of 1–800 nm particles in Helsinki – a street canyon and an urban background station comparison, Atmos. Chem. Phys., 21, 9931–9953, https://doi.org/10.5194/acp-21-9931-2021, 2021.

Olin, M., Kuuluvainen, H., Aurela, M., Kalliokoski, J., Kuittinen, N., Isotalo, M., Timonen, H. J., Niemi, J. V., Rönkkö, T., and Dal Maso, M.: Traffic-originated nanocluster emission exceeds H_2SO_4-driven photochemical new particle formation in an urban area, Atmos. Chem. Phys., 20, 1–13, https://doi.org/10.5194/acp-20-1-2020, 2020.

Olofsson, M., Suikkanen, S., Kobos, J., Wasmund, N., and Karlson, B.: Basin-specific changes in filamentous cyanobacteria community composition across four decades in the Baltic Sea, Harmful Algae, 91, 101685, https://doi.org/10.1016/j.hal.2019.101685, 2020.

Paasonen, P., Nieminen, T., Asmi, E., Manninen, H. E., Petäjä, T., Plass-Dülmer, C., Flentje, H., Birmili, W., Wiedensohler, A., Hõrrak, U., Metzger, A., Hamed, A., Laaksonen, A., Facchini, M. C., Kerminen, V.-M., and Kulmala, M.: On the roles of sulphuric acid and low-volatility organic vapours in the initial steps of atmospheric new particle formation, Atmos. Chem. Phys., 10, 11223–11242, https://doi.org/10.5194/acp-10-11223-2010, 2010.

Petäjä, T., Mauldin III, R. L., Kosciuch, E., McGrath, J., Nieminen, T., Paasonen, P., Boy, M., Adamov, A., Kotiaho, T., and Kulmala, M.: Sulfuric acid and OH concentrations in a boreal forest site, Atmos. Chem. Phys., 9, 7435–7448, https://doi.org/10.5194/acp9-7435-2009, 2009

Peters, C., Pechtl, S., Stutz, J., Hebestreit, K., Hönninger, G., Heumann, K. G., Schwarz, A., Winterlik, J., and Platt, U.: Reactive and organic halogen species in three different European coastal environments, Atmos. Chem. Phys., 5, 3357–3375, https://doi.org/10.5194/acp-5-3357-2005, 2005.

Pierce, J. R., Riipinen, I., Kulmala, M., Ehn, M., Petäjä, T., Junninen, H., Worsnop, D. R., and Donahue, N. M.: Quantification of the volatility of secondary organic compounds in ultrafine particles during nucleation events, Atmos. Chem. Phys., 11, 9019–9036, https://doi.org/10.5194/acp-11-9019-2011, 2011.

Raso, A. R. W., Custard, K. D., May, N. W., Tanner, D., Newburn, M. K., Walker, L., Moore, R. J., Huey, L. G., Alexander, L., Shepson, P. B., and Pratt, K. A.: Active molecular iodine photochemistry in the Arctic, P. Natl. Acad. Sci. USA, 114, 10053–10058, https://doi.org/10.1073/pnas.1702803114, 2017.

Riipinen, I., Yli-Juuti, T., Pierce, J. R., Petäjä, T., Worsnop, D. R., Kulmala, M., and Donahue, N. M.: The contribution of organics to atmospheric nanoparticle growth, Nat. Geosci., 5, 453–458, https://doi.org/10.1038/ngeo1499, 2012.

Rong, H., Liu, J., Zhang, Y., Du, L., Zhang, X., and Li, Z.: Nucleation mechanisms of iodic acid in clean and polluted coastal regions, Chemosphere, 253, 126743, https://doi.org/10.1016/j.chemosphere.2020.126743, 2020.

Rose, C., Zha, Q., Dada, L., Yan, C., Lehtipalo, K., Junninen, H., Mazon, S. B., Jokinen, T., Sarnela, N., Sipilä, M., Petäjä, T., Kerminen, V. M., Bianchi, F., and Kulmala, M.: Observations of biogenic ion-induced cluster formation in the atmosphere, Sci. Adv., 4, 1–11, https://doi.org/10.1126/sciadv.aar5218, 2018.

Saiz-Lopez, A. and Plane, J. M. C.: Novel iodine chemistry in the marine boundary layer, Geophys. Res. Lett., 31, 1999–2002, https://doi.org/10.1029/2003GL019215, 2004.

Saiz-Lopez, A., Plane, J. M. C., Baker, A. R., Carpenter, L. J., Von Glasow, R., Gómez Martín, J. C., McFiggans, G., and Saunders, R. W.: Atmospheric chemistry of iodine, Chem. Rev., 112, 1773–1804, https://doi.org/10.1021/cr200029u, 2012.

Sarnela, N., Jokinen, T., Nieminen, T., Lehtipalo, K., Junninen, H., Kangasluoma, J., Hakala, J., Taipale, R., Schobesberger, S., Sipilä, M., Larnimaa, K., Westerholm, H., Heijari, J., Kerminen, V.-M., Petäjä, T., and Kulmala, M.: Sulphuric acid and aerosol particle production in the vicinity of an oil refinery, Atmos. Environ., 119, 156–166, https://doi.org/10.1016/j.atmosenv.2015.08.033, 2015.

Schade, G. W. and Crutzen, P. J.: Emission of aliphatic-amines from animal husbandry and their reactions: Potential source of N_2O and HCN, J. Atmos. Chem., 22, 319–346, https://doi.org/10.1007/BF00696641, 1995.

Schagerström, E., Forslund, H., Kautsky, L., Pärnoja, M., and Kotta, J.: Does thalli complexity and biomass affect the associated flora and fauna of two co-occurring Fucus species in the Baltic Sea?, Estuar. Coast. Shelf S., 149, 187–193, https://doi.org/10.1016/j.ecss.2014.08.022, 2014.

Simon, M., Dada, L., Heinritzi, M., Scholz, W., Stolzenburg, D., Fischer, L., Wagner, A. C., Kürten, A., Rörup, B., He, X.-C., Almeida, J., Baalbaki, R., Baccarini, A., Bauer, P. S., Beck, L., Bergen, A., Bianchi, F., Bräkling, S., Brilke, S., Caudillo, L., Chen, D., Chu, B., Dias, A., Draper, D. C., Duplissy, J., El-Haddad, I., Finkenzeller, H., Frege, C., Gonzalez-Carracedo, L., Gordon, H., Granzin, M., Hakala, J., Hofbauer, V., Hoyle, C. R., Kim, C., Kong, W., Lamkaddam, H., Lee, C. P., Lehtipalo, K., Leiminger, M., Mai, H., Manninen, H. E., Marie, G., Marten, R., Mentler, B., Molteni, U., Nichman, L., Nie, W., Ojdanic, A., Onnela, A., Partoll, E., Petäjä, T., Pfeifer, J., Philippov, M., Quéléver, L. L. J., Ranjithkumar, A., Rissanen, M. P., Schallhart, S., Schobesberger, S., Schuchmann, S., Shen, J., Sipilä, M., Steiner, G., Stozhkov, Y., Tauber, C., Tham, Y. J., Tomé, A. R., Vazquez-Pufleau, M., Vogel, A. L., Wagner, R., Wang, M., Wang, D. S., Wang, Y., Weber, S. K., Wu, Y., Xiao, M., Yan, C., Ye, P., Ye, Q., Zauner-Wieczorek, M., Zhou, X., Baltensperger, U., Dommen, J., Flagan, R. C., Hansel, A., Kulmala, M., Volkamer, R., Winkler, P. M., Worsnop, D. R., Donahue, N. M., Kirkby, J., and Curtius, J.: Molecular understanding of new-particle formation from α-pinene between -50 and $+25\,^{\circ}C$, Atmos. Chem. Phys., 20, 9183–9207, https://doi.org/10.5194/acp-20-9183-2020, 2020.

Sipilä, M., Berndt, T., Petaja, T., Brus, D., Vanhanen, J., Stratmann, F., Patokoski, J., Mauldin, R. L., Hyvärinen, A. P., Lihavainen, H., and Kulmala, M.: The role of sulfuric acid in atmospheric nucleation, Science, 327, 1243–1246, https://doi.org/10.1126/science.1180315, 2010.

Sipilä, M., Sarnela, N., Jokinen, T., Junninen, H., Hakala, J., Rissanen, M. P., Praplan, A., Simon, M., Kürten, A., Bianchi, F., Dommen, J., Curtius, J., Petäjä, T., and Worsnop, D. R.: Bisulfate – cluster based atmospheric pressure chemical ionization mass spectrometer for high-sensitivity (< 100 ppqV) detection of atmospheric dimethyl amine: proof-of-concept and first ambient data from boreal forest, Atmos. Meas. Tech., 8, 4001–4011, https://doi.org/10.5194/amt-8-4001-2015, 2015.

Sipilä, M., Sarnela, N., Jokinen, T., Henschel, H., Junninen, H., Kontkanen, J., Richters, S., Kangasluoma, J., Franchin, A., Peräkylä, O., Rissanen, M. P., Ehn, M., Vehkamäki, H., Kurten, T., Berndt, T., Petäjä, T., Worsnop, D., Ceburnis, D., Kerminen, V. M., Kulmala, M., and O'Dowd, C.: Molecular-scale evidence of aerosol particle formation via sequential addition of HIO_3, Nature, 537, 532–534, https://doi.org/10.1038/nature19314, 2016.

Sørensen, S., Falbe-Hansen, H., Mangoni, M., Hjorth, J., and Jensen, N. R.: Observation of DMSO and $CH_3S(O)OH$ from the gas phase reaction between DMS and OH, J. Atmos. Chem., 24, 299–315, https://doi.org/10.1007/BF00210288, 1996.

Steinke, M., Hodapp, B., Subhan, R., Bell, T. G., and Martin-Creuzburg, D.: Flux of the biogenic volatiles isoprene and dimethyl sulfide from an oligotrophic lake, Sci. Rep., 8, 630, https://doi.org/10.1038/s41598-017-18923-5, 2018.

Suikkanen, S., Laamanen, M., and Huttunen, M.: Long-term changes in summer phytoplankton communities of the open northern Baltic Sea, Estuar. Coast. Shelf S., 71, 580–592, https://doi.org/10.1016/j.ecss.2006.09.004, 2007.

Suikkanen, S., Pulina, S., Engström-Öst, J., Lehtiniemi, M., Lehtinen, S., and Brutemark, A.: Climate Change and Eutrophication Induced Shifts in Northern Summer Plankton Communities, PLoS One, 8, 1–10, https://doi.org/10.1371/journal.pone.0066475, 2013.

SYKE press release: Summary of algal bloom monitoring June–August 2019: Cyanobacteria were mostly mixed in the water in the Finnish sea areas, in lakes the cyanobacteria situation varied a lot, https://www.syke.fi/en-US/Current/Press_releases/Summary_of_algal_bloom_monitoring_JuneAu(51391), last access: 29 August 2019.

Thakur, R. C., Dada, L., Beck, L. J., Quéléver, L. L. J., Chan, T., Marbouti, M., He, X.-C., Xavier, C., Sulo, J., Lampilahti, J., Lampimäki, M., Tham, Y. J., Sarnela, N., Lehtipalo, K., Norkko, A., Kulmala, M., Sipilä, M., and Jokinen, T.: An evaluation of new particle formation events in Helsinki during a Baltic Sea cyanobacterial summer bloom, Zenodo [data set], https://doi.org/10.5281/zenodo.6426198, 2022.

Torn, K., Krause-Jensen, D., and Martin, G.: Present and past depth distribution of bladderwrack (Fucus vesiculosus) in the Baltic Sea, Aquat. Bot., 84, 53–62, https://doi.org/10.1016/j.aquabot.2005.07.011, 2006.

Tröstl, J., Chuang, W. K., Gordon, H., Heinritzi, M., Yan, C., Molteni, U., Ahlm, L., Frege, C., Bianchi, F., Wagner, R., Simon, M., Lehtipalo, K., Williamson, C., Craven, J. S., Duplissy, J., Adamov, A., Almeida, J., Bernhammer, A. K., Breitenlechner, M., Brilke, S., Dias, A., Ehrhart, S., Flagan, R. C., Franchin, A., Fuchs, C., Guida, R., Gysel, M., Hansel, A., Hoyle, C. R., Jokinen, T., Junninen, H., Kangasluoma, J., Keskinen, H., Kim, J., Krapf, M., Kürten, A., Laaksonen, A., Lawler, M., Leiminger, M., Mathot, S., Möhler, O., Nieminen, T., Onnela, A., Petäjä, T., Piel, F. M., Miettinen, P., Rissanen, M. P., Rondo, L., Sarnela, N., Schobesberger, S., Sengupta, K., Sipilä, M., Smith, J. N., Steiner, G., Tomè, A., Virtanen, A., Wagner, A. C., Weingartner, E., Wim-

mer, D., Winkler, P. M., Ye,P., Carslaw, K. S., Curtius, J., Dommen, J., Kirkby, J., Kulmala, M., Riipinen, I., Worsnop, D. R., Donahue, N. M., and Baltensperger, U.: The role of low-volatility organic compounds in initial particle growth in the atmosphere, Nature, 26, 527–531, https://doi.org/10.1038/nature18271, 2016.

Väkevä, M., Hämeri, K., Puhakka, T., Nilsson, E. D., Hohti, H., and Mäkelä, J. M.: Effects of meteorological processes on aerosol particle size distribution in an urban background area, J. Geophys. Res.-Atmos., 105, 9807–9821, https://doi.org/10.1029/1999JD901143, 2000.

Vanhanen, J., Mikkilä, J., Lehtipalo, K., Sipilä, M., Manninen, H. E., Siivola, E., Petäjä, T., and Kulmala, M.: Particle size magnifier for nano-CN detection, Aerosol Sci. Tech., 45, 533–542, https://doi.org/10.1080/02786826.2010.547889, 2011.

Wagner, R., Manninen, H. E., Franchin, A., Lehtipalo, K., Mirme, S., Steiner, G., Petäjä, T., and Kulmala, M.: On the accuracy of ion measurements using a Neutral cluster and Air Ion Spectrometer, Boreal Environ. Res., 21, 230–241, 2016.

Wang, Z., Wu, Z., Yue, D., Shang, D., Guo, S., Sun, J., Ding, A., Wang, L., Jiang, J., Guo, H., Gao, J., Cheung, H. C., Morawska, L., Keywood, M., and Hu, M.: New particle formation in China: Current knowledge and further directions, Sci. Total Environ., 577, 258–266, https://doi.org/10.1016/j.scitotenv.2016.10.177, 2017.

Wang, Z. B., Hu, M., Yue, D. L., Zheng, J., Zhang, R. Y., Wiedensohler, A., Wu, Z. J., Nieminen, T., and Boy, M.: Evaluation on the role of sulfuric acid in the mechanisms of new particle formation for Beijing case, Atmos. Chem. Phys., 11, 12663–12671, https://doi.org/10.5194/acp-11-12663-2011, 2011.

Weber, R. J., McMurry, P. H., Mauldin, L., Tanner, D. J., Eisele, F. L., Brechtel, F. J., Kreidenweis, S. M., Kok, G. L., Schillawski, R. D., and Baumgardner, B.: A study of new particle formation and growth involving biogenic and trace gas species measured during ACE 1, J. Geophys. Res.-Atmos., 103, 16385–16396, https://doi.org/10.1029/97JD02465, 1998.

Weber, R. J., McMurry, P. H., Mauldin, R. L., Tanner, D. J., Eisele, F. L., Clarke, A. D., and Kapustin, V. N.: New particle formation in the remote troposphere: A comparison of observations at various sites, Geophys. Res. Lett., 26, 307–310, https://doi.org/10.1029/1998GL900308, 1999.

Wimmer, D., Buenrostro Mazon, S., Manninen, H. E., Kangasluoma, J., Franchin, A., Nieminen, T., Backman, J., Wang, J., Kuang, C., Krejci, R., Brito, J., Goncalves Morais, F., Martin, S. T., Artaxo, P., Kulmala, M., Kerminen, V.-M., and Petäjä, T.: Ground-based observation of clusters and nucleation-mode particles in the Amazon, Atmos. Chem. Phys., 18, 13245–13264, https://doi.org/10.5194/acp-18-13245-2018, 2018.

Yan, C., Yin, R., Lu, Y., Dada, L., Yang, D., Fu, Y., Kontkanen, J., Deng, C., Garmash, O., Ruan, J., Baalbaki, R., Schervish, M., Cai, R., Bloss, M., Chan, T., Chen, T., Chen, Q., Chen, X., Chen, Y., Chu, B., Dällenbach, K., Foreback, B., He, X., Heikkinen, L., Jokinen, T., Junninen, H., Kangasluoma, J., Kokkonen, T., Kurppa, M., Lehtipalo, K., Li, H., Li, H., Li, X., Liu, Y., Ma, Q., Paasonen, P., Rantala, P., Pileci, R. E., Rusanen, A., Sarnela, N., Simonen, P., Wang, S., Wang, W., Wang, Y., Xue, M., Yang, G., Yao, L., Zhou, Y., Kujansuu, J., Petäjä, T., Nie, W., Ma, Y., Ge, M., He, H., Donahue, N. M., Worsnop, D. R., Veli-Matti, K., Wang, L., Liu, Y., Zheng, J., Kulmala, M., Jiang, J., and Bianchi, F.: The Synergistic Role of Sulfuric Acid, Bases, and Oxidized Organics Governing New-Particle Formation in Beijing, Geophys. Res. Lett., 48, e2020GL091944, https://doi.org/10.1029/2020GL091944, 2021.

Yao, L., Garmash, O., Bianchi, F., Zheng, J., Yan, C., Kontkanen, J., Junninen, H., Mazon, S. B., Ehn, M., Paasonen, P., Sipilä, M., Wang, M., Wang, X., Xiao, S., Chen, H., Lu, Y., Zhang, B., Wang, D., Fu, Q., Geng, F., Li, L., Wang, H., Qiao, L., Yang, X., Chen, J., Kerminen, V. M., Petäjä, T., Worsnop, D. R., Kulmala, M., and Wang, L.: Atmospheric new particle formation from sulfuric acid and amines in a Chinese megacity, Science, 361, 278–281, https://doi.org/10.1126/science.aao4839, 2018.

Yu, H., Ren, L., Huang, X., Xie, M., He, J., and Xiao, H.: Iodine speciation and size distribution in ambient aerosols at a coastal new particle formation hotspot in China, Atmos. Chem. Phys., 19, 4025–4039, https://doi.org/10.5194/acp-19-4025-2019, 2019.

Zhang, R., Wang, L., Khalizov, A. F., Zhao, J., Zheng, J., McGraw, R. L., and Molina, L. T.: Formation of nanoparticles of blue haze enhanced by anthropogenic pollution, P. Natl. Acad. Sci. USA, 106, 17650–17654, https://doi.org/10.1073/pnas.0910125106, 2009.

Zheng, G., Kuang, C., Uin, J., Watson, T., and Wang, J.: Large contribution of organics to condensational growth and formation of cloud condensation nuclei (CCN) in the remote marine boundary layer, Atmos. Chem. Phys., 20, 12515–12525, https://doi.org/10.5194/acp-20-12515-2020, 2020.

Zheng, J., Hu, M., Zhang, R., Yue, D., Wang, Z., Guo, S., Li, X., Bohn, B., Shao, M., He, L., Huang, X., Wiedensohler, A., and Zhu, T.: Measurements of gaseous H_2SO_4 by AP-ID-CIMS during CAREBeijing 2008 Campaign, Atmos. Chem. Phys., 11, 7755–7765, https://doi.org/10.5194/acp-11-7755-2011, 2011.